Observer Based Open Transistor Fault Diagnosis and Fault-Tolerant Control of Five-Phase PM Motor Drive for Application in Electric Vehicles

Journal:	*IET Power Electronics*
Manuscript ID:	PEL-2013-0949.R1
Manuscript Type:	Research Paper
Date Submitted by the Author:	16-Apr-2014
Complete List of Authors:	Salehifar, Mehdi; Universitat Polytechnica de Catalunya, Electronic Engineering Moreno-Eguilaz, Juan Manuel; Universidad Politecnica de Catalunya, Electronics Salehi, Ramin; Universitat Polytechnica de Catalunya, Electronic Engineering Sala, Vicent; Universitat Polytechnica de Catalunya, Electronic Engineering Romeral Martinez, Jose Luis; Universidad Politecnica de Catalunya, Electronics
Keyword:	FAULT DIAGNOSIS, MOTOR DRIVES, DC-AC POWER CONVERTORS

Dear editor,

Thank you very much for agreeing to review the following manuscript:

Manuscript Title: “Observer Based Open Transistor Fault Diagnosis and Fault-Tolerant Control of Five-Phase PM Motor Drive for Application in Electric Vehicles”

Manuscript Number: PEL-2013-0949

We would like to thank the Reviewers, as well as the Associated Editor, for giving us guidance with their helpful comments.

As suggested by the editor, a throughout revision of the paper has been carried out and the comments of the reviewers have been properly answered in the current version of the manuscript. Significant changes made on the original version of the manuscript appear highlighted in color text in the current version. Below you can find the author’s response.

Reviewer: 1

Comments to the Author:

The paper describes an online method for open-circuit fault diagnosis in PM drives.

The method is model based, and as such uses a comparison of model/observer estimation and measured data. The error between the observed and measured stator currents are used to drive the parameter (L and R) estimation.

1. It is not clear how (14) can decouple the estimation of the phase self (L) and mutual (M) inductances of the model (1)-(3)

As it has been truly mentioned by reviewer, in case of available mutual inductances, (14) cannot decouple the self and mutual inductances.

From design point of view, in order to increase reliability of a fault-tolerant multiphase PM machine, the mutual inductances should be minimized in comparison to self inductances [R1-R2]. Due to this fact, and small effect of mutual inductances given in (1) and (3), this parameter can be neglected in the model.

In this paper, mutual inductances are neglected. Therefore, (14) can truly estimate the phase inductances.

This has been explained in the new version of the manuscript.

Also, mutual inductance of five-phase BLDC motor used in experimental setup in this paper is 18 µH, and its self inductance is 408 µH. As it can be seen, mutual inductance is only 3.6 % of self inductance. Therefore it can be neglected.

Modifications in the new version of the manuscript (i.e. Section II – Page5) have been highlighted with yellow color.

[R1] M. Villani, M. Tursini, G. Fabri, and L. Castellini: 'High Reliability Permanent Magnet Brushless Motor Drive for Aircraft Application', IEEE Trans. Ind. Electron., 2012, 59, (5), pp. 2073-2081

[R2] T. Raminosoa, C. Gerada, and M. Galea: 'Design Considerations for a Fault-Tolerant Flux-Switching Permanent-Magnet Machine', IEEE Trans. Ind. Electron, 2011, 58, (7), pp. 2818-2825

2. The purpose of the observer (16)-(20) is very unclear. The authors state that the open loop model (after parameter adaptation) is compared with the measured current and any difference is attributed to faults ("The error signal increases remarkably"). Then they include the observer (16)-(18) whose purpose is to drive the current error to zero using the current error as an input?

According to the control method shown in Fig. R1, two observers have been designed in this paper.

The aim of the first observer (denoted by observer 1 in Fig. R1) is to estimate the motor parameters (i.e. R and L). The observer type is adaptive; details are given in section III.A in manuscript. The equations (14)-(15) are used to realize this observer.

On the other side, another observer (denoted by observer 2 in Fig. R1) is designed only to estimate the motor phase currents. The observer type is a sliding mode observer (SMO); details are given in section III.C in manuscript. This observer needs the parameters of the motor (i.e. R and L) known. Here estimated parameters by the adaptive parameter estimator are used. As a result, an ideal model of the motor is used in the SMO observer. It means that estimated current by the ideal model and real currents are equal. Details of the SMO are given in section III.C. The equations (16)-(18) are used to realize SMO. The equation (19)-(20) are used to evaluate the stability of the SMO given in (16)-(18).

The error signal available in SMO (i.e. the difference between real and estimated current denoted by δ in the manuscript) is compared to a threshold value which is equal to zero. It should be noted that under healthy mode operation of the motor, δ value is near zero. In the case that δ value is higher than threshold, a fault alarm is generated.

After fault alarm, fault detection (FD) and localization is done by the algorithm given in section IV of the manuscript. Here this algorithm is shown in Fig. R2. Inputs to the FD block are real current and estimated current by SMO. At the same time, parameter estimation using the first observer (denoted by Observer 1 in Fig. R1) is stopped. Since there is a fault in the inverter, the estimated parameters by model are no longer accurate. Here parameters are updated with values during one cycle before the fault.

The necessity of both observers has been highlighted in the section III – Page5. It is mentioned that the comparison between δ and threshold value is used to generate the fault alarm in section III.C – Page7 - Paragraph 2.

Also, Fig. 3(a) in the manuscript was updated as shown in Fig. R1 to show clearly:

- The observers,
- Inputs to each observer,
- Comparison between δ and threshold value and
- Fault diagnosis block.

The modifications in the new version of the manuscript are highlighted with yellow color. Here, the modifications are also shown in Fig. R1.

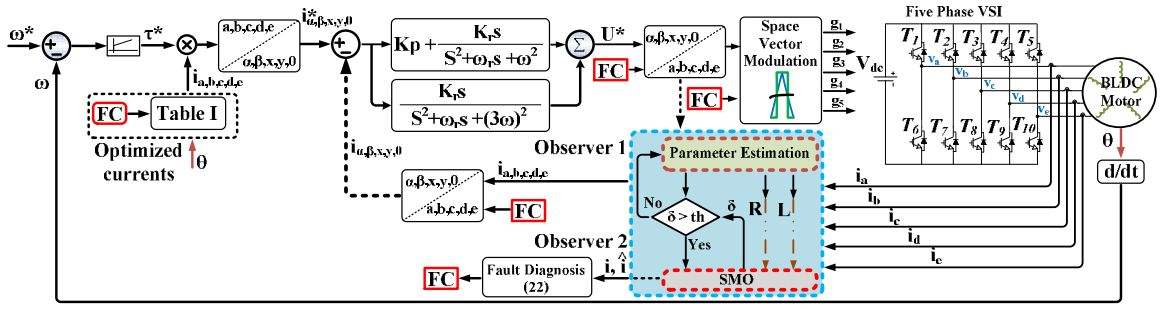

Fig. R1. Fault detection, parameter identification and Fault-Tolerant FOC

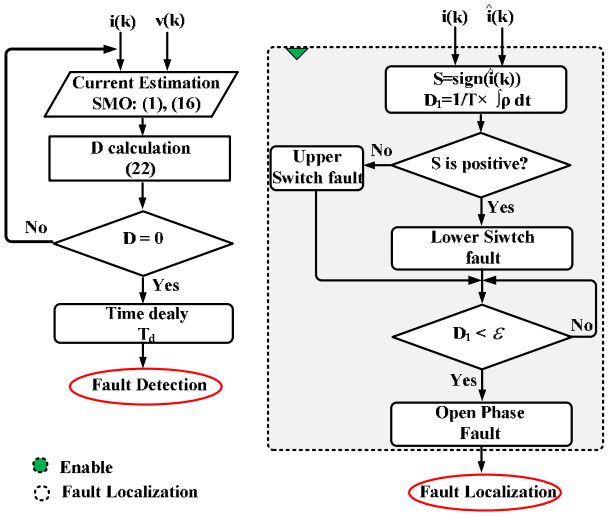

Fig. R2. FD and localization method.

3. What kind of average is mu in (21)? Is it a moving average?

As it has been correctly mentioned by the reviewer, a moving average is used in (21) to calculate cross correlation factor. This has been mentioned in the new version of the manuscript.

Modifications have been highlighted with yellow color in Section IV – Page 9.

4. Why is a PR controller used? The authors state that "PI controller is limited due to low bandwidth" and then the PR has "same transient and steady state response similar to PI" ? In general a PR in stationary coordinates is equivalent to a PI in rotating coordinates.

According to field oriented control (FOC) algorithm of the five-phase motor drive shown in Fig. R1, two control loops are used. An outer controller is used to set the motor reference speed. Since motor speed is a dc value, this controller is realized by using a simple PI controller.

An inner controller is also used to set the motor reference currents. In this paper, PR controller is used to implement the inner controller.

In order to justify the application of PR controller, motor reference phase currents in abcde frame are shown under healthy and faulty conditions in Fig. R3(a). Besides, current references in synchronous reference frame (i.e. after applying Park's transformation to abcde frame currents) are shown in Fig. R3(b). As it can be seen from Fig. R3(b), reference currents at synchronous reference frame under faulty mode are no longer pure dc components. Both the first and third harmonics appear in the reference currents in synchronous reference frame. Also, reference currents in abcde frame are unbalanced and nonsinusoidal.

According to literature [R3-R6], PI controllers are the best choice for controlling dc components. In case of sinusoidal reference currents, PI controller cannot track reference currents in steady state due to finite gain [R7]. There will be steady state error.

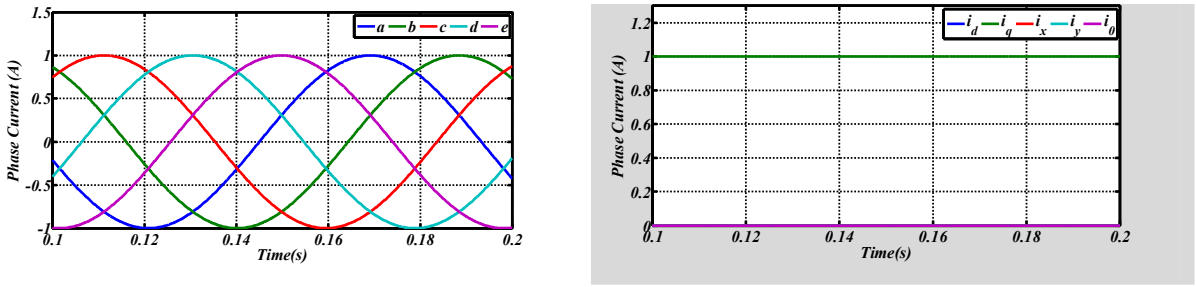

Healthy phase currents

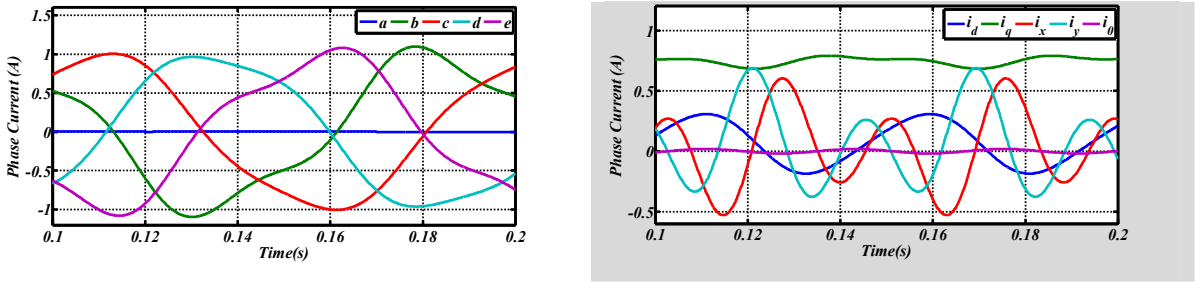

One faulty phase currents (i_a=0)

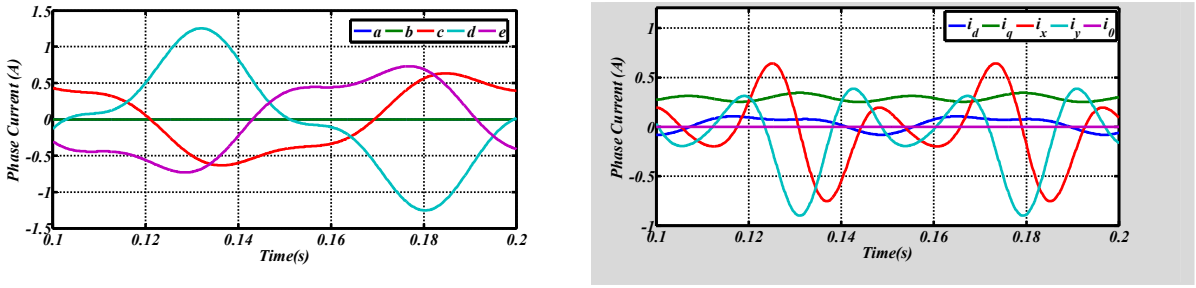

Two adjacent faulty phase currents (i_a=0, i_b=0)

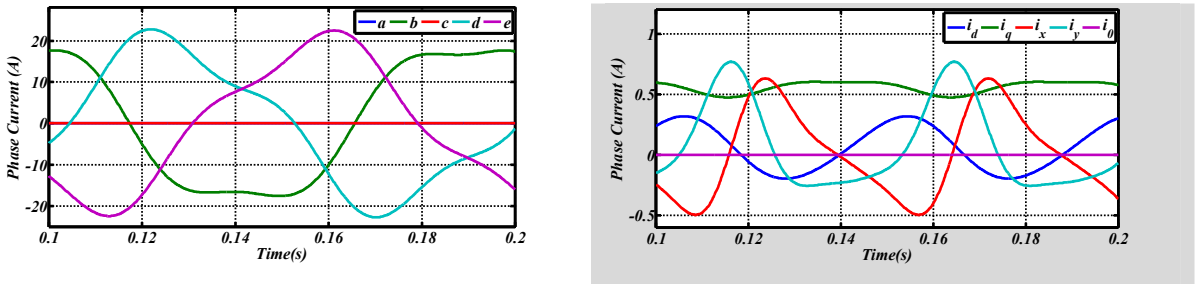

Two nonadjacent faulty phase currents (i_a=0, i_c=0)

(a) (b)

Fig. R3. Reference currents in (a) abcde frame. (b) in synchronous reference frame.

In case of a five-phase BLDC motor at synchronous reference frame, reference currents are dc components only under healthy mode control; this can be seen clearly in Fig. R3(b). While under faulty mode, phase currents are nonsinusoidal and unbalanced.

A comprehensive study has been done on different current controllers in [R7]. According to [R7], in order to achieve zero steady state error using a PI controller in synchronous reference frame, following design steps should be considered in the case of a five-phase BLDC motor as:

1- Design a PI controller for dc components

2- Design a PI controller in each synchronous frame for each individual harmonic

3- Since currents are unbalanced under faulty mode, the controller should be designed for both positive and negative sequence components, separately.

By considering steps 1-3, the reference currents in synchronous reference frame will be dc values. Here, PI controller can be used to achieve zero steady state error.

However this approach leads to a complicated controller design.

A simple alternative can be a proportional controller plus sinusoidal controllers at each harmonic frequency at stationary reference frame. This controller type is known as proportional resonant (PR) controller in literature [R7]. It has following advantages:

1- It can be used to control both positive and negative sequence components at the same time.

2- Each harmonic component in phase current can be controlled individually without affecting other components.

It should be noted that it is advantages to supply a multiphase drive by fundamental and harmonics in phase current [R8]. This control method has advantage of increased torque produced by the machine and reduced toque ripple. For example in case of a five-phase machine, phase currents consist of both first and third harmonics. In case of seven phase machine, phases currents consist of first, third and fifth harmonics. Consequently, to achieve a zero steady sate error in a fault tolerant five-phase BLDC machine using conventional PI controller, a complicated design is necessary.

To further remark the advantage of using the PR controller, a simple comparison has been done between PI and PR controller as shown in Fig. R4.

As it can be seen from Fig. R4, due to its simple implementation, less calculation and zero steady state error, in this paper, PR controller is used to control the reference currents of the motor.

The advantages of using the PR controller and its characteristics have been thoroughly explained in the new version of the manuscript (i.e. Section V – Pages 11-13). The new modifications have been highlighted with blue color.

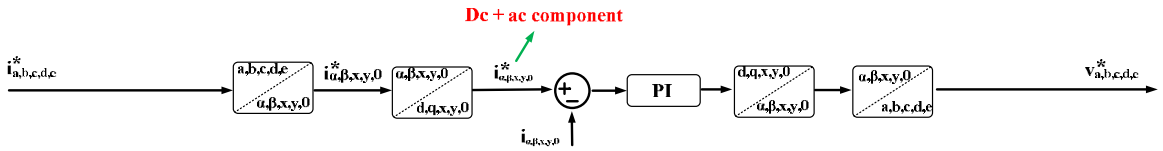

(a) conventional PI controller

Disadvantage: steady state error due to ac components

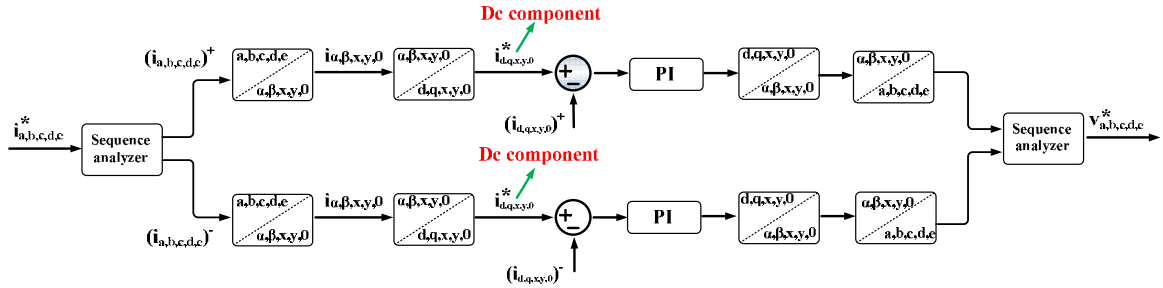

(b) improved PI controller

Disadvantage: high computational cost

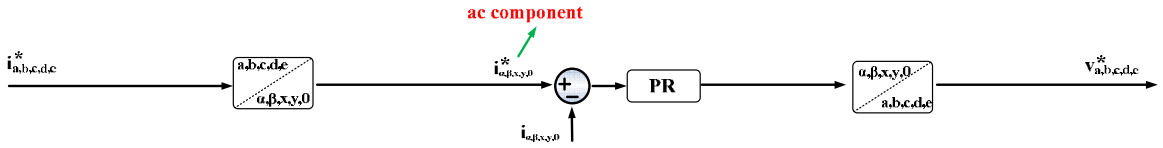

(c) PR controller

Fig. R4. Comparison between PI and PR controllers to implement the inner controller of the five-phase BLDC motor.

[R3] Yaoqin Jia, Jiqian Zhao, and Xiaowei Fu: 'Direct Grid Current Control of LCL-Filtered Grid-Connected Inverter Mitigating Grid Voltage Disturbance', IEEE Trans. Power Electron., 2014, 29, (3), pp. 1532-1541

[R4] Ana Vidal, F. D. Freijedo, A. G. Yepes, P. Fernandez-Comesana, J. Malvar, O. Lopez, and J. Doval-Gandoy: 'Assessment and Optimization of the Transient Response of Proportional-Resonant Current Controllers for Distributed Power Generation Systems', IEEE Trans. Ind. Electron., 2013, 60, (4), pp. 1367-1383

[R5] Chenlei Bao, Xinbo Ruan, Xuehua Wang, Weiwei Li, Donghua Pan, and Kailei Weng: 'Step-by-Step Controller Design for LCL-Type Grid-Connected Inverter with Capacitor–Current-Feedback Active-Damping', IEEE Trans. Power Electron., 2014, 29, (3), pp. 1239-1253.

[R6] Changyue Zou, Bangyin Liu, Shanxu Duan and Rui Li: 'Stationary Frame Equivalent Model of Proportional-Integral Controller in dq Synchronous Frame', IEEE Trans. Power Electron., 2014, To be published.

[R7] L. Rodrigues Limongi, R. Bojoi, G. Griva, and A. Tenconi: 'Comparing the Performance of Digital Signal Processor-Based Current Controllers for Three-Phase Active Power Filters', IEEE Ind. Electron. Mag., 2009, Digital Object Identifier 10.1109/MIE.2009.931894

[R8] Leila Parsa, and Hamid A. Toliyat: 'Five-Phase Permanent-Magnet Motor Drives', IEEE Trans. Ind. Appl., 2005, 41, (1), pp. 30-37.

5. "According to a recent survey..." please include a reference.

According to the reviewer's comments, the corresponding reference [R9] was included in the new version of the manuscript.

Modifications are highlighted with yellow color in the reference section.

[R9] Shaoyong Yang, Angus Bryant, Philip Mawby, Dawei Xiang, Li Ran, and Peter Tavner: 'An Industry-Based Survey of Reliability in Power Electronic Converters', IEEE Trans. Ind. Appl., 2011, 47, (3), pp. 1441-1451

6. Please thoroughly revise the English of your paper. Many sentences are unclear, e.g.

"First fault is a single switch type",

According to the reviewer's comment, the English language of the paper was thoroughly revised.

New modifications in the text are highlighted with blue text color.

Reviewer: 2

Comments to the Author

1. **More details about the control circuit and the type of DSP or µP used.**

A dSPACE model ds1005 is used to implement the control algorithm of the five-phase BLDC motor and fault diagnosis method. Details of the controller have been mentioned in **section VI – Page 13** of the manuscript.

On the other side, the five-phase BLDC motor is coupled with a commercial three-phase PMSM as the load. The load motor is supplied with an independent AC SIEMENS drive (known as SINAMICS-S120). A national instrument card known as Compactrio is used as interface between the three phase PMSM drive and the host PC. The torque and speed commands of the load motor are sent to commercial drive by host PC.

More explanation about the experimental setup has been included in the new version of the manuscript. The new modifications are highlighted with blue color in the new version of the manuscript (**i.e. section VI– Page 13**).

The fault-tolerant field oriented control algorithm of the five-phase BLDC motor drive is shown in Fig. R5(a). As seen, control algorithm consists of a speed controller (i.e. the outer controller which has been realized by a simple PI controller) and a current controller (i.e. the inner controller which has been realized by a PR controller).

To further explain the control circuit, the following modifications have been done in the new version of the manuscript (**i.e. section V**).

- More details about each one of the speed and current controllers have been presented.

- Current references of the five-phase motor under healthy and faulty mode are presented in **table I** in manuscript.

- A comparison between PI and PR controller is done, and advantages of using PR controller to implement the inner current controller are highlighted.

- The equations of PR controller and its characteristics are discussed.

- The modifications of the control circuit under each operation mode of the machine are also shown in Fig. R5(b).

These modifications are highlighted in section V of the manuscript with blue color.

Also, design of the PR controller is thoroughly discussed in section VI.A of the manuscript. Relevant references (i.e [R10]-[R13]) are also added to the reference list.

The modifications are highlighted with blue color in the new version of the manuscript.

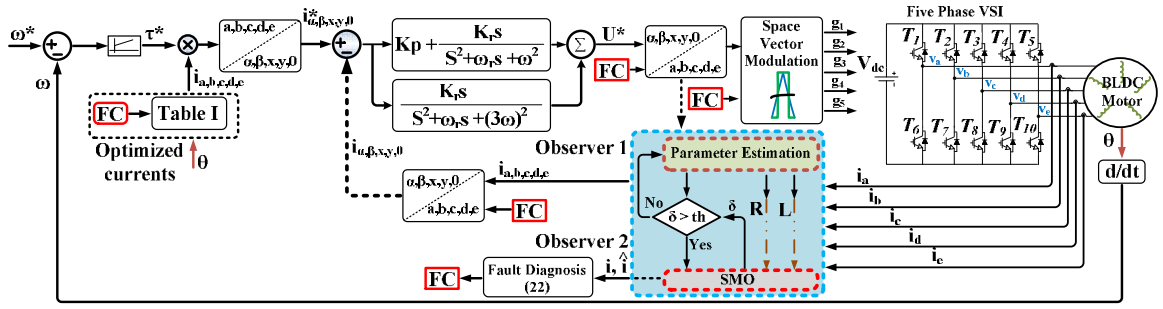

(a)

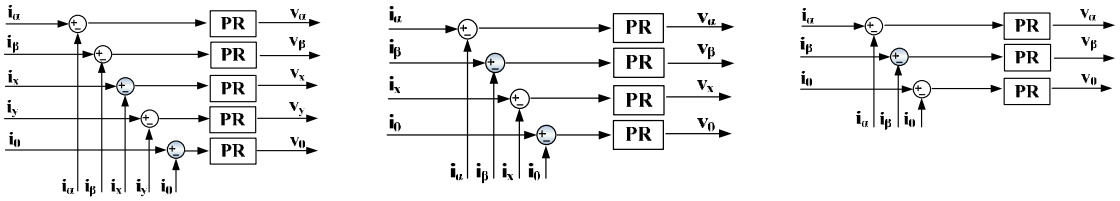

Healthy mode One faulty phase mode Two faulty phase mode

(b)

Fig. R5. (a) Fault detection, parameter identification and Fault-Tolerant FOC (b) Block diagram of the inner current controller under each operational mode of the motor.

TABLE I
Optimized phase currents with isolated neutral

Current	A	B	C	D	E
one faulty phase (FC=2)					
I_1(PU)	0	0.99	0.99	1	0.98
θ_1	-	51	137	232	-41
I_3(PU)	0	0.17	0.08	0.09	0.19
θ_3	-	23	52	186	-19
two adjacent faulty phases (FC=3)					
I_1(PU)	0	0	0.59	0.95	0.67
θ_1	-	-	82	218	0
I_3(PU)	0	0	0.12	0.29	0.16
θ_3	-	-	44	102	41
two nonadjacent faulty phases (FC=4)					
I_1(PU)	0	0.99	0	0.98	0.99
θ_1	-	77	-	2	-42
I_3(PU)	0	0.16	0	0.19	0.17
θ_3	-	15	-	55	-21

[R10] L. Rodrigues Limongi, R. Bojoi, G. Griva, and A. Tenconi: 'Comparing the Performance of Digital Signal Processor-Based Current Controllers for Three-Phase Active Power Filters', IEEE Ind. Electron. Mag., 2009, Digital Object Identifier 10.1109/MIE.2009.931894

[R11] A. G. Yepes, F. D. Freijedo, J. Doval-Gandoy, O. Lopez, J. Malvar, and P. Fernandez-Comesana: 'Effects of Discretization Methods on the Performance of Resonant Controllers', IEEE Trans. Power Electron., 2010, 25, (7), pp. 1692-1712

[R12] Chenlei Bao, Xinbo Ruan, Xuehua Wang, Weiwei Li, Donghua Pan, and Kailei Weng: 'Step-by-Step Controller Design for LCL-Type Grid-Connected Inverter with Capacitor–Current-Feedback Active-Damping', IEEE Trans. Power Electron., 2014, 29, (3), pp. 1239-1253

[R13] D. G. Holmes, T. A. Lipo, B. P. McGrath, and W. Y. Kong: 'Optimized Design of Stationary Frame Three Phase AC Current Regulators', IEEE Trans. Power Electron., 2009, 24, (11), pp. 2417-2426

Observer Based Open Transistor Fault Diagnosis and Fault-Tolerant Control of Five-Phase PM Motor Drive for Application in Electric Vehicles

Mehdi SALEHIFAR[1], Ramin Salehi ARASHLOO[2], Manuel MORENO-EGUILAZ[3], Vicent SALA[4], Luis ROMERAL[5]

[1] **CORRESPONDING AUTHOR,** mehdi.salehifar@mcia.upc.edu

[2] ramin.salehi@mcia.upc.edu,

[3] juan.manuel.moreno@mcia.upc.edu

[4] vicent.sala@mcia.upc.edu

[5] Luis.Romeral@mcia.upc.edu

All Authors are with Electronic Engineering Department, UPC, Rambla Sant Nebridi, s/n, 08222 Terrassa, Spain, Tel. +34 633402065, Fax. +34 93 739 89 72

Abstract **– to meet increasing demand for higher reliability in power electronics converters applicable in electric vehicles, fault detection (FD) is an important part of the control algorithm. In this paper, a model based open transistor fault diagnosis method is presented for a voltage-source inverter (VSI) supplying a five-phase PM motor drive. To realize this goal, a model based observer is designed to estimate model parameters. After that, the estimated parameters are used to design a sliding mode observer (SMO) in order to estimate the phase current in an ideal model. Subsequently, the proposed FD technique measures the similarity between the estimated current and real current using cross correlation factor. This factor is used for the first time in this paper to define a FD index in VSI. The presented FD scheme is simple and fast; also, it is able to detect multiple open switch or open phase faults in contrast to conventional methods. On the other side, in order to track reference current of the motor, the estimated parameters are used to design a proportional resonant (PR) controller. The FD technique is used to operate a multiphase fault-tolerant brushless direct current (BLDC) motor drive. Experimental results on a five-phase BLDC motor with in-wheel outer rotor applicable in electrical vehicles are conducted to validate the theory.**

Keyword – fault diagnosis, multiphase fault-tolerant BLDC motor drive, sliding mode observer, cross correlation.

I. INTRODUCTION

Nowadays, power converters are widely used in industrial applications. Along the rising applications, there is an increasing demand for higher reliability provided by the power electronic systems in applications such as transportation, electric and hybrid electric vehicle, space craft, and more electric aircraft. Fault-tolerant concept is an economic solution to meet this requirement [1]. To accomplish a fault-tolerant system, three main subjects should be considered at the same time in the final design including fault-tolerant design, control and fault diagnosis.

Multiphase fault-tolerant permanent magnet (PM) motor drive is a unique solution to achieve high reliability [2]. In the case of a five-phase motor, it is possible to maintain the operation with two faulty phases. Regarding this solution, it is necessary to supply the motor with a fault-tolerant converter. The fault-tolerant converter should be able to detect and isolate the faulty components.

According to a recent survey on reliability of power electronics converters [3], power switches are the most vulnerable components in a power converter among others. A complete review of the faulty modes and detection methods in a power converter was conducted in [4]. Open switch and short circuit faults are the most common faults in a power switch among others. The short circuit fault should be detected and removed quite fast; otherwise it can damage the whole system. Nowadays, hardware based methods are frequently included in commercial gate driver to protect against this fault. On the other side, a solution to detect and protect the open switch fault is not available in commercial products. If it is not detected, secondary faults may happen. Due to growing demand for higher reliability by industry, an extensive research has been conducted on open switch FD methods, recently. Regarding the presented open switch FD methods in literature, these methods can be considered in three different categories including signal based methods, reference based methods and model based methods.

The signal based FD schemes have been extensively studied in literature. To realize a signal based FD method, the current or voltage signal of the power converter can be used as an input to the FD block. The detection methods based on the voltage signal need extra hardware to detect the fault; as a result, implementation of these methods is expensive. However these methods are able to detect the fault very fast. Such schemes have been presented in [5-6].

The FD methods based on the current signal have also been extensively addressed in literature. Different schemes using tools such as Park's vector modulus, wavelet transform, dc current method, normalized dc current method, Fourier transform and slope method have been presented to obtain a suitable FD index [4]. Low detection speed, complexity, inability to detect multiple faults, and sensitivity to fast load transients are the main drawbacks of FD methods based on the current signal. In this category, proposed methods in [7-9] show the highest performance among others.

The second type of the open switch FD method is based on the reference current. According to this method, real current of the converter is measured and compared to the reference current in the control algorithm. After that, a FD index is defined based on

the residue value. This method is cheap, fast and robust to the variations of load parameters. Estima et al. [10] presented a FD method based on the reference current. This method cannot be used in a system with open loop control.

The third type of the open switch FD method is based on the system model. According to this technique, the input signal to the plant is applied to an equivalent mathematical model of the plant, and its response is predicted. In the next step, difference between real output and the predicted signal is used to define the FD index [11-15]. This method is cheap, since extra hardware is not necessary for FD. A FD method based on observer has been presented in [14] to detect multiple open switch faults in a three-phase induction motor. A bank of observers has been proposed to detect the fault. Consequently, implementation of this method will be even more complicated in the case of a multiphase converter. Shao et al. [16] have presented an open switch FD method based on SMO for application in a modular multilevel converter. In order to detect the fault, the residue value (i.e. the difference between estimated and real signal) is compared with a fixed threshold value. This approach can lead to false alarm, since FD index is not independent from load operational conditions.

Regarding the model based FD methods, and to overcome the limitations discussed above, a model based FD method is presented in this paper. Based on this method, in the first step the phase currents are estimated by a full state SMO in a fault-tolerant five-phase BLDC motor drive. Comparing to conventional model based methods which use the residue value (i.e. the difference between measured and estimated state) to define FD index, here cross correlation technique is proposed to define this index. Inputs to the cross correlation technique are the measured and estimated current of the power converter. Proposed method still has the advantages of the conventional methods. At the same time, it can effectively detect multiple open switch or open phase faults. Furthermore, it is quite robust to transients and parameter uncertainties. An estimator is also designed to estimate the motor parameters. The estimated parameters are used for two purposes. These two purposes are SMO design and the PR controller design.

The major contribution of this paper is developing a model based open transistor FD method. To present the FD technique, the remainder of this paper is organized as follows. The model of the five-phase BLDC motor is explained in section II. The current estimation using SMO is presented in section III. Proposed FD scheme is presented in section IV. The FD method is included in a fault-tolerant control algorithm; theory is presented in section V. Proposed FD method is used to detect different faulty modes in a five-phase VSI supplying a BLDC motor; experimental results are shown for both FD and fault-tolerant control in section VI. And finally, the conclusions and remarkable points are presented in section VII.

II. Model of Five-Phase BLDC Motor

The proposed FD technique in this paper intends to implement fault diagnosis in a five-phase VSI supplying a BLDC motor drive, as shown in Fig. 1. Field oriented control (FOC) is used to control the motor; inputs to the control algorithm consist of the phase currents and rotor mechanical position. The same inputs are sent to the FD block. After FD, this block decides the

operation mode (i.e. healthy or faulty) of the motor. In order to isolate the fault, it is necessary to remove the gate signal of the switch in the faulty leg.

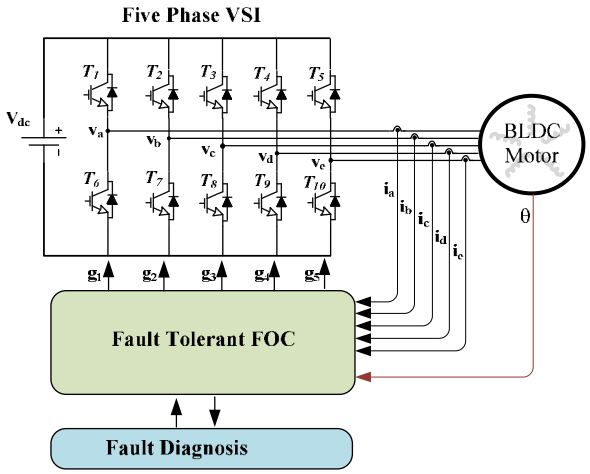

Fig. 1. Fault-Tolerant BLDC motor drive.

To implement FD method, in the first step motor phase currents are estimated based on well-known models. The model in ABCDE reference frame is used due to its less computational requirements and simpler modelling specially under faulty mode. The model of the five-phase BLDC motor with trapezoidal back EMF under healthy and faulty modes is:

$$\begin{bmatrix} v_a \\ v_b \\ v_c \\ v_d \\ v_e \end{bmatrix} = \begin{bmatrix} R_a & 0 & 0 & 0 & 0 \\ 0 & R_b & 0 & 0 & 0 \\ 0 & 0 & R_c & 0 & 0 \\ 0 & 0 & 0 & R_d & 0 \\ 0 & 0 & 0 & 0 & R_e \end{bmatrix} \begin{bmatrix} i_a \\ i_b \\ i_c \\ i_d \\ i_e \end{bmatrix} + \begin{bmatrix} L_a & M_1 & M_2 & M_2 & M_1 \\ M_1 & L_b & M_1 & M_2 & M_2 \\ M_2 & M_1 & L_c & M_1 & M_2 \\ M_2 & M_2 & M_1 & L_d & M_1 \\ M_1 & M_2 & M_2 & M_1 & L_e \end{bmatrix} \frac{d}{dt} \begin{bmatrix} i_a \\ i_b \\ i_c \\ i_d \\ i_e \end{bmatrix} + \begin{bmatrix} e_a \\ e_b \\ e_c \\ e_d \\ e_e \end{bmatrix} - v_x \begin{bmatrix} 1 \\ 1 \\ 1 \\ 1 \\ 1 \end{bmatrix}. \quad (1)$$

where i is the phase current, v is the terminal voltage of each phase, R is the equivalent phase resistance, L is the equivalent phase inductance, M_1 is mutual inductance between two adjacent phases, M_2 is mutual inductance between two nonadjacent phases, e is the back EMF in each phase of the motor, and v_x is the neutral voltage of the motor. The back EMF will be estimated as follows:

$$\begin{bmatrix} e_a \\ e_b \\ e_c \\ e_d \\ e_e \end{bmatrix} = \lambda_{m1}\omega_e \begin{bmatrix} \cos(\vartheta) \\ \cos(\vartheta - 2\pi/5) \\ \cos(\vartheta - 4\pi/5) \\ \cos(\vartheta - 6\pi/5) \\ \cos(\vartheta - 8\pi/5) \end{bmatrix} + \lambda_{m3}\omega_e \begin{bmatrix} \cos(3\vartheta) \\ \cos 3(\vartheta - 2\pi/5) \\ \cos 3(\vartheta - 4\pi/5) \\ \cos 3(\vartheta - 6\pi/5) \\ \cos 3(\vartheta - 8\pi/5) \end{bmatrix}. \quad (2)$$

where λ_{m1} and λ_{m3} are the first and third harmonic amplitudes of the rotor flux linkage; ω_e is the electrical rotational velocity, and ϑ is the rotor electrical angle.

To simplify the model under healthy and faulty modes, the model in (1) is redefined in terms of voltage difference between machine terminals as follow:

(3)

$$\begin{bmatrix} v_{ab} \\ v_{bc} \\ v_{cd} \\ v_{de} \end{bmatrix} = \begin{bmatrix} R_a - R_b & 0 & 0 \\ 0 & R_b - R_c & 0 \\ 0 & 0 & R_c & -R_d \\ R_e & R_e & R_e & R_d + R_e \end{bmatrix} \begin{bmatrix} i_a \\ i_b \\ i_c \\ i_d \end{bmatrix} + \begin{bmatrix} e_{ab} \\ e_{bc} \\ e_{cd} \\ e_{de} \end{bmatrix} + \begin{bmatrix} L_a + M_2 - 2M_1 & M_2 - L_b & 2M_2 - 2M_1 & M_2 - M_1 \\ M_1 - M_2 & L_b - M_1 & M_1 - L_c & M_2 - M_1 \\ M_1 - M_2 & 2M_1 - 2M_2 & L_c - M_2 & 2M_1 - M_2 - L_d \\ L_e + M_2 - 2M_1 & L_e - M_1 & L_e - M_2 & L_e + L_d - 2M_1 \end{bmatrix} \frac{d}{dt} \begin{bmatrix} i_a \\ i_b \\ i_c \\ i_d \end{bmatrix}.$$

From design point of view, in order to increase the reliability of a multiphase fault-tolerant machine, the mutual inductances should be minimized [17]. Due to this fact, and because of small effect of mutual inductances given in (1) and (3), this parameter in the model is neglected in the rest of this paper. It should be noted that under faulty mode, the corresponding row and column of the faulty phase are eliminated from (1). After that, the motor model can be simply redefined in terms of voltage difference between machine terminals similar to (3).

The model presented in (3) is utilized to estimate the phase currents and model parameters. The signal estimation methods based on the load model are sensitive to parameter uncertainties and non modeled dynamics [14]. Consequently, to estimate the phase currents accurately, a full state SMO is applied to the open loop model. Due to the observer, the error between real and estimated state variable converges to zero under healthy mode. Details of the designed observer are explained in the next section.

III. Accurate Current Estimation Using SMO

As discussed above, the motor phase currents are estimated based on the motor model. The current estimation is realized using two separate observers. An observer is used to estimate model parameters in (3). Other observer (i.e. SMO) is used to estimate motor phase currents; the estimated motor parameters are used in the SMO. Therefore, the motor model used in the SMO is an ideal model.

If the motor parameters are known accurately, then estimated currents using the open loop model will be equal to the real current. However, these parameters are not easily accessible. On the other hand, parameter values can change with temperature and operational condition of the motor. Furthermore, for condition monitoring and control purposes, it is desirable to calculate machine parameters online.

In order to diagnose the fault and design the PR controllers, the motor parameters are estimated in this paper. Estimation method is explained in the next section.

A. Stator's Parameter Estimation

In a BLDC motor, the stator parameters (i.e. phase resistance and inductance) have a high effect on the accuracy of the open loop model. An estimator is designed to calculate the parameters. The basic equations of the machine model given in (1) can be rewritten as:

$$\frac{d}{dt}i_j = -A_j i_j + B(v_j - e_j),\ \ j = a,b,c,d,e. \qquad (4)$$

where $A=R/L$ and B=$1/L$. The goal is to estimate A and B.

In order to improve the estimation accuracy of the open loop model, a nonlinear model reference adaptive observer is designed to estimate the parameters. Estimated currents are as:

$$\frac{d}{dt}\hat{i}_j = -\hat{A}\hat{i}_j + \hat{B}(v_j - e_j), \qquad j = a,b,c,d,e. \qquad (5)$$

where ^ is used to denote the estimated components.

B. STABILITY ANALYSIS

In order to ensure the stability of the estimation algorithm and to design the observers, a stability analysis is done. Here Lyapunov function is used to ensure stability of the system and measurement of parameters. This function is defined as:

$$V = \frac{1}{2}S^2 + \frac{1}{2}(\hat{A} - A)^2 + \frac{1}{2}(\hat{B} - B)^2. \qquad (6)$$

where S is an error function. There are different possibilities to choose the error function [18]. The error function used in this paper is as follows:

$$S = \delta + \lambda \int \delta dt. \qquad (7)$$

where δ is equal to difference between the estimated and real current in each phase of the power converter, and λ is a positive constant. If the error is equal to zero (i.e. S=0), then, the observer is no longer sensitive to parameter uncertainties. Taking into account (1) and (7), the derivative of S for the first element is calculated as:

$$\dot{S} = \dot{\delta} + \lambda\delta. \qquad (8)$$

$$\dot{\delta}_a = \dot{\hat{i}}_a - \dot{i}_a = (A - \hat{A})\hat{i}_a - A\delta_a + (v_a - e_a)(\hat{B} - B). \qquad (9)$$

where $\dot{}$ is equivalent to dx/dt. Similarly, other components are calculated.

According to Lyapunov stability theory, if derivative of V is less than zero for all positive V values, then the system is stable [19]. The derivative of (6) is as:

$$\dot{V} = S^T\dot{S} + (\hat{A} - A)\dot{\hat{A}} + (\hat{B} - B)\dot{\hat{B}}. \qquad (10)$$

From (9) and (10), the derivative of V function can be computed as:

$$\begin{aligned}\dot{V} &= (\delta_a + \lambda\int\delta_a)\times -(A - \lambda)\delta_a \\ &+ ((\delta_a + \lambda\int\delta_a)\times(A - \hat{A})\hat{i}_a + (\hat{A} - A)\dot{\hat{A}}) \\ &+ ((\delta_a + \lambda\int\delta_a)\times(v_a - e_a)(\hat{B} - B) + (\hat{B} - B)\dot{\hat{B}}).\end{aligned} \qquad (11)$$

The first element in (11) is negative for λ values less than A. According to Lyapunov stability condition, the remaining components can be calculated as:

$$\dot{\hat{A}} = (\delta_a + \lambda \int \delta_a) \times \hat{i}_a \qquad (12)$$

$$\dot{\hat{B}} = -(\delta_a + \lambda \int \delta_a) \times (v_a - e_a) \qquad (13)$$

Under steady state condition, the error and its dynamic are zero. So, the resistance and inductance can be calculated from (12)-(13) as follows:

$$\frac{1}{\hat{L}} = \frac{1}{L} - \int (\delta_a + \lambda \int \delta_a) \times (v_a - e_a) dt. \qquad (14)$$

$$\hat{R} = R + \hat{L} \int (\delta_a + \lambda \int \delta_a) \times \hat{i}_a. \qquad (15)$$

From (14) and (15), instantaneous values of R and L can be calculated. In this paper, the estimated parameters are used to design the PR controller and to estimate the phase currents using a SMO.

As aforementioned, the estimated parameters can be used for other purposes such as improving the controller of the motor. For example in the case of using a predictive controller in a BLDC motor, it is possible to have both good transient and steady state performance; however the controller performance is sensitive to parameter uncertainties. Therefore, the parameter estimation can be used to design a robust predictive controller. Detection of high resistance connection in cables feeding the machine has been presented in [20], [21].

In order to detect a fault in VSI, the phase currents of the motor are predicted; a SMO is used for this purpose. The estimated parameters in (14)-(15) are used in the SMO. Details of SMO are presented in the following section.

C. Current Estimation

In order to estimate the phase currents, SMO is used in this paper. It has many advantages which make it a suitable option for the state variable estimation. Simple implementation, robustness to parameter uncertainty and measurement noise are the most important factors among others [16].

As it was shown above, a model reference adaptive observer was used to estimate motor parameters. Since real parameters are already known from the parameter estimator, response of the open loop model should be equal to real current. In the case of a healthy motor, error signal reduces to zero after few cycles. In presence of a fault, the model based estimator can no longer estimate the parameters accurately. Under this condition, the error signal increases remarkably.

To detect a fault, the error signal available in SMO is compared to a threshold above zero. If it increases beyond the threshold, a fault alarm is generated. Since the estimated parameters are no longer accurate in a faulty motor, the estimated values are always memorized during one cycle before the fault alarm. After the fault alarm, the controller and model parameters are updated with estimated values for one cycle before the fault.

To estimate the phase currents accurately, the SMO is designed as:

$$\begin{bmatrix} L_a & -L_b & 0 & 0 \\ 0 & L_b & -L_c & 0 \\ 0 & 0 & L_c & -L_d \\ L_e & L_e & L_e & L_e + L_d \end{bmatrix} \frac{d}{dt} \begin{bmatrix} \hat{i}_a \\ \hat{i}_b \\ \hat{i}_c \\ \hat{i}_d \end{bmatrix} = \begin{bmatrix} v_{ab} - e_{ab} \\ v_{bc} - e_{bc} \\ v_{cd} - e_{cd} \\ v_{de} - e_{de} \end{bmatrix} - \begin{bmatrix} R_a - R_b & 0 & 0 \\ 0 & R_b - R_c & 0 \\ 0 & 0 & R_c & -R_d \\ R_e & R_e & R_e & R_d + R_e \end{bmatrix} \begin{bmatrix} \hat{i}_a \\ \hat{i}_b \\ \hat{i}_c \\ \hat{i}_d \end{bmatrix} - K \times Sat\left(\begin{bmatrix} \delta_a \\ \delta_b \\ \delta_c \\ \delta_d \end{bmatrix} \right). \quad (16)$$

where K is the observer gain, and Sat is a saturation function defined as follows:

$$Sat(x) = \begin{cases} 1 & x \geq 1 \\ x & -1 < x < 1 \\ -1 & x \leq -1 \end{cases} \quad (17)$$

It is possible to use different functions instead of Sat such as *Sigmoid* and *Sign* function. The high frequency oscillations can be avoided in the estimated variables, if the saturation function in (17) is used. In order to obtain suitable values of K, a stability analysis is presented in the following section.

To evaluate stability of the SMO, Lyapunov function is defined as:

$$V = \frac{1}{2} S^2. \quad (18)$$

The Lyapunov function and its derivative given in (9)-(10) are similarly adapted here. Taking into account (1) and (18), the derivative of δ for the first element is calculated as:

$$\dot{\hat{\delta}}_a = \dot{\hat{i}}_a - \dot{i}_a = -\frac{R_a}{L_a}(\hat{i}_a - i_a) - \frac{K}{L_a} \times Sat(\hat{i}_a - i_a). \quad (19)$$

Similarly, other components are calculated. So, derivative of V function is as:

$$\dot{V} = [\delta_a \ \delta_b \ \delta_c \ \delta_d \ \delta_e]^T \times \begin{bmatrix} -\frac{R_a}{L_a}\delta_a - \frac{K}{L_a} \times Sat(\delta_a) \\ -\frac{R_b}{L_b}\delta_b - \frac{K}{L_b} \times Sat(\delta_b) \\ -\frac{R_c}{L_c}\delta_c - \frac{K}{L_c} \times Sat(\delta_c) \\ -\frac{R_d}{L_d}\delta_d - \frac{K}{L_d} \times Sat(\delta_d) \\ -\frac{R_e}{L_e}\delta_e - \frac{K}{L_e} \times Sat(\delta_e) \end{bmatrix}. \quad (20)$$

Since Sat function is a linear function, sign of $\delta_a Sat(\delta_a)$ will be always positive. Consequently, the only condition to achieve sliding surface is for positive K values. According to (19), by choosing higher values of K, dynamic behaviour of resultant error will be even faster.

It should be noted that K value has a significant effect on the performance of the proposed FD method. If a very high value is chosen for K, the observed value will follow the real state too fast. Therefore, the residue value will be low. On the other hand, by choosing a small value for K, the estimated current will still follow the current pattern before the fault. In this case, it is easier to detect the fault, since the faulty current is significantly different from the healthy current. A low value of K is an optimal choice in this paper. This assumption results in a robust SMO with slow dynamics. This claim will be later validated with experimental results.

IV. Fault Diagnostic Method

In order to detect the fault, it is possible to define a simple FD index (i.e. the error between the estimated and real current values). Developing this approach for a multiphase machine can lead to false alarms. The main reasons are explained in details in the following.

When a fault occurs in one phase of the converter, closed loop control tries to minimize the error between the reference currents and real currents. As a result, in case that the healthy control method is still applied, output voltage of the control block for a faulty inverter will be changed. On the other hand, in the case of a single switch fault in one phase, a dc value is added to the remaining healthy phase currents. In the case of multiple open switch faults, the dc value can be very high. Consequently, due to effect of the control method, and faulty signals, the estimated currents in the remaining healthy phases can be different from the real values. In addition, simplifications in model can result in a small error. If estimated and real current values are different, this error can be interpreted as a false alarm based on the error value. As a result, FD block should be robust to these cases. These effects will be later validated by experimental results.

To overcome the drawbacks of a simple FD index based on the error function, an alternative solution is proposed in this paper. Here the estimated and measured current signals are fed to a simple unique algorithm. The presented algorithm can detect both the single switch and open phase faults in a VSI. According to this algorithm, the similarity level between two input current signals is measured as a function of time; this measuring factor is known as cross correlation [22]. This factor is defined as:

$$\rho_{x_1-x_2}=\frac{\sum_{j=1}^{N}(x_{1j}-\bar{\mu}_{x1})(x_{2j}-\bar{\mu}_{x2})}{\sqrt{\sum_{j=1}^{N}(x_{1j}-\bar{\mu}_{x1})^2\sum_{j=1}^{N}(x_{2j}-\bar{\mu}_{x2})^2}}. \qquad (21)$$

where x_1 and x_2 are the estimated and measured current in each phase of the power converter, respectively; μ is the moving average value of the input variables and N is the number of samples. It is worth to note that, N value determines the evaluation period in each sampling point. Choosing a small value for N makes the ρ value sensitive to noise. On the other side, a high N value enlarges the detection time. Moreover, the ρ value will be sensitive to frequency transients in a variable speed drive. It

should be noted that the smallest value for N is one sample in one period; the highest value is the number of samples in one period of a fundamental frequency. So, a tradeoff should be done between sensitivity to noise and FD speed.

The ρ value varies from -1 to 1. In the case of completely similar waveforms, its value approaches to 1. According to (21), under healthy condition in a motor drive, both the estimated and real currents are similar, so the correlation factor is near 1. However under faulty mode, these waveforms are quite different at least for half of one fundamental cycle. Under faulty mode, the cross correlation factor reduces to zero. So, the ρ factor is a suitable index to distinguish a healthy condition from a faulty condition.

In comparison to the conventional methods, the proposed method is robust to all false alarms due to fast load transients or unbalanced nonsinusoidal waveforms. Consequently, a FD index is defined as:

$$D = \rho. \qquad (22)$$

The D value is equal to zero under faulty mode, while it is close to 1 under healthy mode. Therefore, D value equal to zero indicates a fault condition. To improve the robustness of the proposed FD method against noise and fast transients, here FD is done with a small time delay denoted by t_d. If the D value is equal to zero during t_d, then the open switch or open phase fault is detected.

After FD, it is necessary to locate the faulty component in VSI. The fault scenario in one leg of VSI can be either a single switch fault or an open phase fault. Due to the single switch fault, average value of the phase current during one fundamental cycle is positive in the case of a lower switch fault or negative in the case of an upper switch fault. In the case of the open phase fault, the phase current and ρ factor are zero. Therefore, fault localization in the case of single switch fault is as:

$$sign(\hat{i}) = \begin{cases} > 0 & lower\ switch\ fault \\ < 0 & upper\ switch\ fault \end{cases} \qquad (23)$$

Here the estimated current is used to localize the faulty switch. In order to localize the open phase fault, average value of the ρ factor is calculated during one period as:

$$D_{1j} = \frac{1}{M}\sum_{j=1}^{M}\rho_j, \quad j\varepsilon\{a,b,c,d,e\}. \qquad (24)$$

where M is number of samples in one period. If the average value is zero, then the fault type is an open phase fault. For the sake of simplicity, aforementioned fault types are codified. The fault codes are 1, -1 and 2 in the case of upper switch fault, lower switch fault and open phase fault, respectively. These codes are the same in the rest of this paper. Block diagram of the FD method is shown in Fig. 2. In this figure, ε is a small positive value near to zero.

Based on the presented technique, fault localization in the case of a single switch fault is done during one sampling time after FD. Nonetheless, a time delay around one fundamental cycle is necessary to localize the open phase fault. As it can be seen from

Fig. 2, once the fault is detected, fault localization block is enabled. It should be noted that, the FD is done separately in each phase of the power converter. As a result, the presented FD technique can be applied to any two-level multiphase VSI.

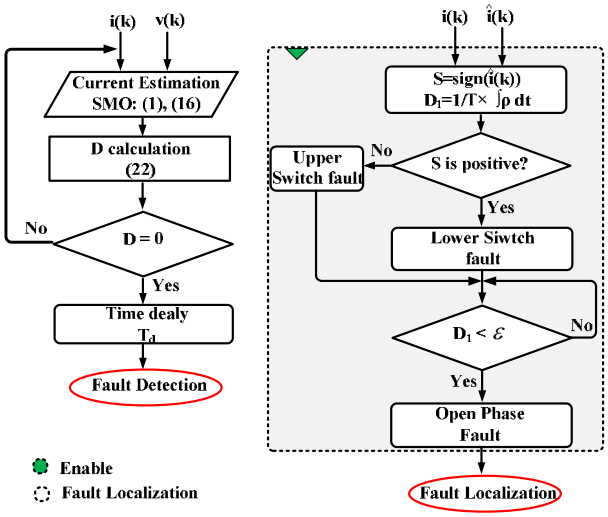

Fig. 2. FD and localization method.

V. Fault-Tolerant Control and Analysis of a Five-Phase BLDC Motor

Application area in this paper is electric vehicles. High reliability is of paramount importance for this application. Five-phase fault-tolerant BLDC motor can meet this requirement. In this paper, fault diagnosis and fault-tolerant control of a multiphase BLDC motor are studied. Block diagram of the studied setup is shown in Fig. 3(a). This motor can be operated with one and two-faulty phases. For clarification, motor operational modes are shown with a code denoted by FC in Fig. 3(a). The operational control mode of the machine is determined by the FD block developed in section IV. Here, control modes of the machine are shown by codes 1, 2, 3, and 4 which correspond to healthy mode, one faulty phase mode, two-adjacent faulty phase mode and two-nonadjacent faulty phase mode, respectively. In the following part, the principals of the fault-tolerant control are briefly reviewed.

In order to control the motor, FOC technique is used. The control algorithm is implemented under healthy and each faulty mode, separately. The basic rules used to calculate the reference currents under different fault conditions were shown in [23]. The calculated reference currents in [23] are shown in Table I. As it can be seen, both first and third harmonics are included in the reference currents. The reference currents are used in this paper in order to realize the fault-tolerant FOC algorithm.

As it can be seen from Fig. 3(a), to implement FOC algorithm, two controllers are used. An outer controller is used to set the motor reference speed shown by ω^*. A proportional-integrator (PI) controller is typically used to realize the speed controller. In addition, an inner controller is used to set the motor reference currents shown by i^*.

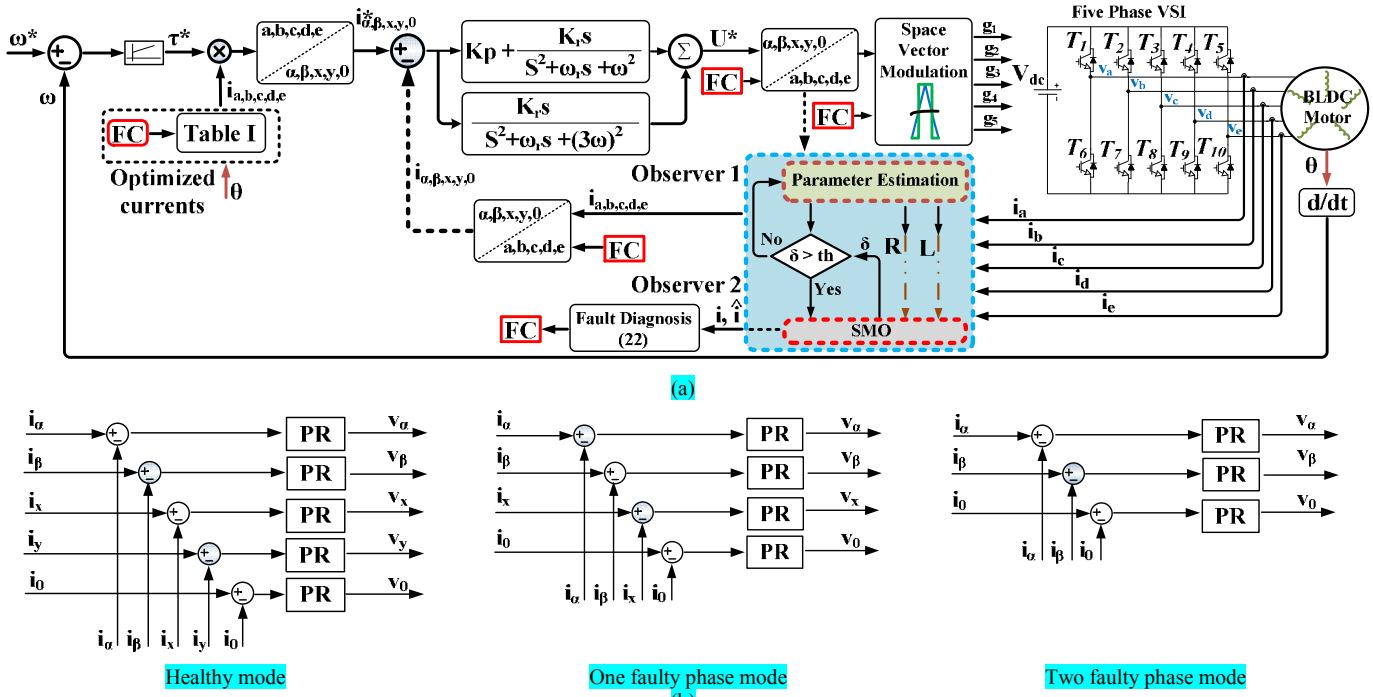

Fig. 3. (a) Fault detection, parameter identification and Fault-Tolerant FOC (b) Block diagram of the inner current controller under each operational mode of the motor.

TABLE I
OPTIMIZED PHASE CURRENTS WITH ISOLATED NEUTRAL

Current	A	B	C	D	E
one faulty phase (FC=2)					
I_1(PU)	0	0.99	0.99	1	0.98
θ_1	-	51	137	232	-41
I_3(PU)	0	0.17	0.08	0.09	0.19
θ_3	-	23	52	186	-19
two adjacent faulty phases (FC=3)					
I_1(PU)	0	0	0.59	0.95	0.67
θ_1	-	-	82	218	0
I_3(PU)	0	0	0.12	0.29	0.16
θ_3	-	-	44	102	41
two nonadjacent faulty phases (FC=4)					
I_1(PU)	0	0.99	0	0.98	0.99
θ_1	-	77	-	2	-42
I_3(PU)	0	0.16	0	0.19	0.17
θ_3	-	15	-	55	-21

The output of the speed controller shown in Fig. 3(a) is the reference torque denoted by τ^*. One main assumption to calculate the optimized reference current values in [23] was no ripples in the generated torque. Therefore, authors here use the conventional PI control to set the reference speed.

Inner controller can be done in different ways. A comprehensive study has been done on different current controllers in [24]. *PI* controller in synchronous reference frame and *PR* controller in stationary reference frame are two possible control methods to set the reference currents. Regarding the optimized reference currents given in table I, under faulty mode, the phase currents are unbalanced and nonsinusoidal. In the case of using a simple *PI* controller, due to unbalanced nonsinusoidal phase currents, both dc component and oscillatory components appear in reference currents after transferring to synchronous reference frame. In order

to have dc reference currents, *PI* controller should be designed separately for positive and negative sequence components. This implies high computational cost and complicated controller design. Furthermore, *PI* controller should be able to track harmonic components as well. It is known in literature that *PI* controller has a high performance to track dc components [24], [25]. In the case of sinusoidal components; there will be steady state error. Therefore, the second disadvantage of *PI* control is poor tracking performance due to its limited bandwidth.

As shown in Fig. 3(a), in this paper, *PR* controller in stationary reference frame is used to implement the inner current controller. According to [24], this controller is able to set both positive and negative sequence components at the same time. On the other hand, resonant controllers can be set individually to track each desired harmonic component. In order to track the reference currents in a five-phase BLDC motor, *PR* controller should be able to control both the first and third harmonics.

Transfer function of *PR* controller is as:

$$G_c(s) = K_p + \frac{K_r s}{s^2 + \omega_r s + \omega_o^2} + \frac{K_r s}{s^2 + \omega_r s + (3\omega_o)^2} \quad (25)$$

where $\omega_o=2\pi f_o$, and f_o is the resonance frequency of the controller, K_p is the proportional gain, K_r is the resonant gain, and ω_r is the bandwidth of the controller around the resonance frequency. It should be noted that ω_r is used to reduce the controller sensitivity at resonance frequency. This criterion should be considered in variable speed drives due to speed variations of the motor. Also, f_o is determined from the motor speed.

As aforementioned, a five-phase BLDC motor can be operated with two faulty phases. This means that inverter configuration under healthy mode, one faulty phase mode, and two faulty phase mode are the five-phase, four-phase, and three-phase, respectively. So, the inner current controller should be reconfigured under each operational mode of the machine. The inner current control scheme at each mode is shown in Fig. 3(b). It should be noted that the Park's transformation should also be updated for five-phase, four-phase or three-phase currents at each operational mode of the machine.

VI. Experimental Results

To validate the theory, experimental results are conducted on a five-phase BLDC motor as shown in Fig. 4. As it can be seen, the five-phase motor is coupled with a commercial three-phase permanent magnet synchronous motor (PMSM) which serves as the load motor. The load motor is supplied with an independent AC SIEMENS drive (known as SINAMICS-S120). A national instrument card known as Compactrio is used as interface between the three phase PMSM drive and the host PC. The torque and speed references of the load motor can be set from the host PC. The five-phase motor parameters are shown in table II. It has an outer rotor in-wheel structure; this configuration is useful for electric vehicles. The control algorithm, and FD method of the five-phase motor are implemented in a dSPACE control board model ds1005. The motor is supplied with a five-phase two level VSI.

The sampling frequency of the phase currents is 4 kHz. The dc link voltage of the VSI is 24 V and its switching frequency is 4 kHz. Motor speed is 23.8 rpm, and rated frequency of the phase currents is 10 Hz.

The experimental results are presented in three sections. In the first section, the motor model is tuned with estimated parameters. After that, the effect of K value on FD performance is discussed. Moreover, characteristics of FD method for application in a multiphase machine will be explained. In the second section, different faulty types are implemented in the inverter; FD method is used to detect and localize the faults. In the last section, the fault-tolerant control of a five-phase BLDC motor is presented; here the FD block is used to achieve the fault-tolerant operation.

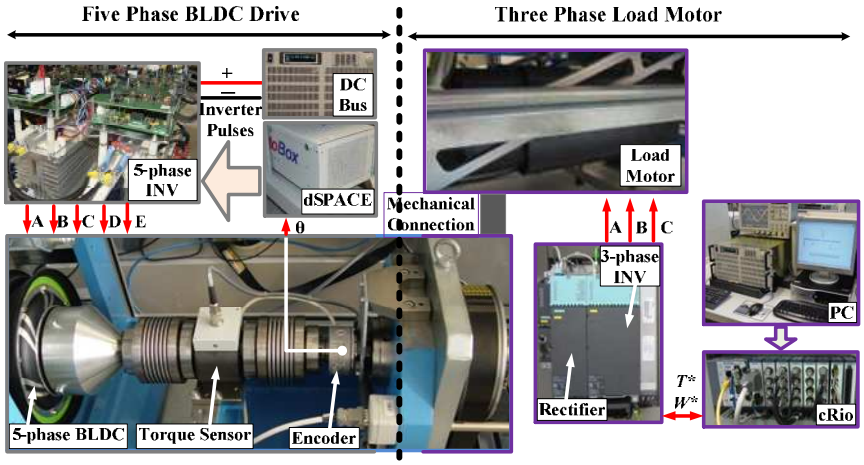

Fig. 4. Experimental setup.

TABLE II
MOTOR PARAMETERS

Number of Pole Pairs		26
Stator Resistance		0.1 Ω
Stator Inductance	L_{aa}	408 μH
	L_{ab}	15 μH
	L_{ac}	18 μH
Nominal Torque		8 Nm
Nominal Speed		400 rpm
Permanent Magnet Flux		0.0178 Wb
Moment of Inertia		0.0583 kgm^2

A. Model Verification

In order to tune the open loop model, in the first step, the presented algorithm in section III is implemented to estimate the stator resistance and inductance of the five-phase BLDC motor. The estimated parameters during four fundamental cycles are shown in Fig. 5(a). As it can be seen, the resistance and inductance value are 0.75 Ω and 490 μH, respectively. To validate effectiveness of the developed theory, a 0.25 Ω resistance was connected in series with phase a. After a short time, it is short circuited. Experimental result of the stator resistance estimation is shown in Fig. 5(b). As it can be seen, the presented parameter estimator can accurately measure the added value.

In the second step, after parameter estimation, the calculated values are used to design the PR controller. Details of the controller design are discussed in the following.

Different methods have been presented in literature to design the PR controllers. In comparison to PI controller, here by adding a resonance term in parallel to a proportional term, the frequency response is only affected around the resonance frequency. The bandwidth of the controller given in (25) at the resonance frequency is defined by integrator term. The proportional gain can be designed similar to *PI* controllers. A similar gain can be chosen for both the first and third harmonics [26]. As a result, the controller design is only considered for the first harmonic.

In order to eliminate the high frequency noise, and at the same time to have a fast dynamic response, the cut off frequency shown by ω_c in this paper is determined well above the resonance frequency [27]. Typical applications consider 1/5 of the switching frequency as the design specification. On the other side, to reduce the controller sensitivity around the resonance frequency, the ω_r value in (25) should be different from zero. In this paper, the design specification is to set ω_r at 0.0628 rad/s, and ω_c at 600 Hz.

Using the estimated parameters, the PR controller is designed according the design method presented in [28]. A block diagram of the inner current controller is shown in Fig. 6(a). Regarding the controller design specifications, the phase margin was considered higher than 45 degrees. Limited value of the motor operation speed for experimental setup is considered as 50 rpm; frequency of the motor phase current at this speed is 21.6 Hz. The designed values for K_p, K_r are 0.067, and 25.27, respectively. The frequency response of the designed PR controller is shown in Fig. 6(b). As it can be seen, the controller has a high gain at the resonance frequency. Therefore, the controller can effectively track both the first and third harmonic components of the motor phase current.

In the third step, the effect of *K* value on FD algorithm is evaluated. two case studies are considered for different values of *K*. For the first case, single switch FD is studied for a low and a high *K* value. Experimental results are shown in Fig. 7(a). The estimated current, real current and error signal are shown. As it can be seen, for small *K* values, the error signal is significantly high. For the second case, open phase FD is evaluated. The final waveforms are shown in Fig. 7(b). As it can be seen, in case of small *K* value, the error signal is high. Consequently, a low value of *K* equal to 4 is considered in this paper which is the same in the rest of this paper.

As discussed before, faulty signals, inaccurate model, and control method performance can affect the estimated current in the remaining healthy phases. To validate this claim, two faulty scenarios are considered here. In the first case, an open switch fault in phase *a*, and an open phase fault in phase *b* are considered. The estimated current, real current and error value in phase *d* are shown in Fig. 7(c). As it can be seen, regardless of being a healthy phase, there is a dc value in phase *d* current. At the same time, the error value during half of one period is high. If the error is used as the FD index, false alarms can be generated in this phase.

To further validate this claim, three lower switch faults are considered in phases *a*, *b*, and *c*. The phase *e* current and error value are shown in Fig. 7(d). Although there is no fault in this phase, the estimated and real current are different.

The presented analysis validates the necessity of a high performance FD method which is robust to these effects. As described above, the FD index presented in (22) in this paper has this characteristic.

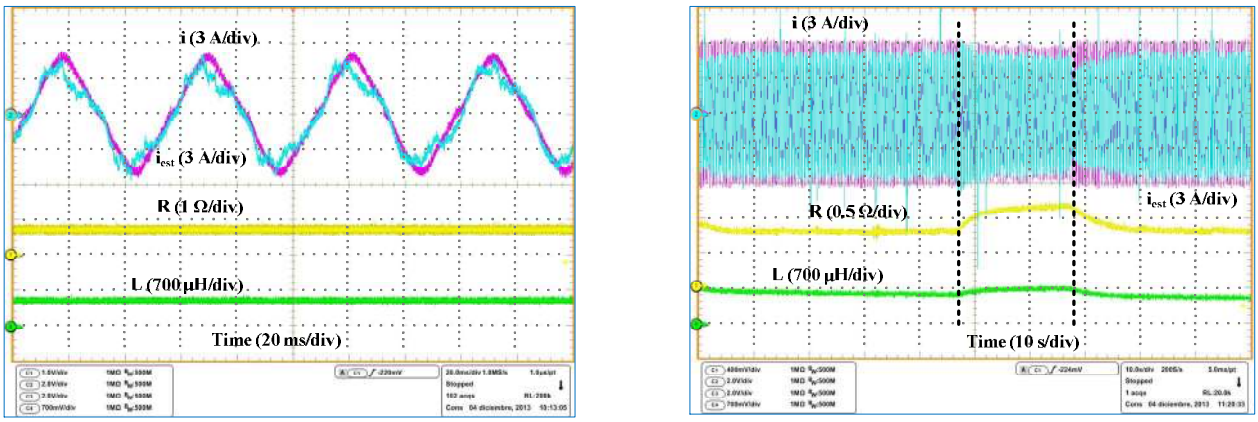

(a) (b)

Fig. 5. Estimated resistance of the stator. (a) Results during four cycles. (b) Results for long time.

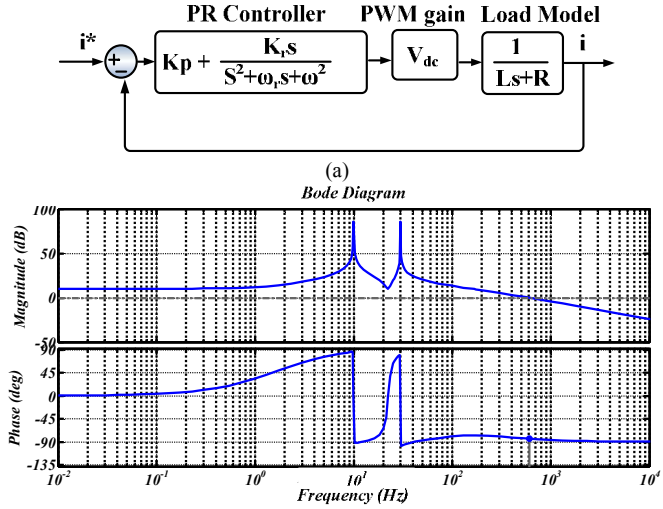

(a)

(b)

Fig. 6. (a) Block diagram of the current controller (b) frequency of the current controller and its frequency response at ω_c=3768 (rad/sec), ω_r=0.0628 (rad/sec) and ω_o=62.8 (rad/sec).

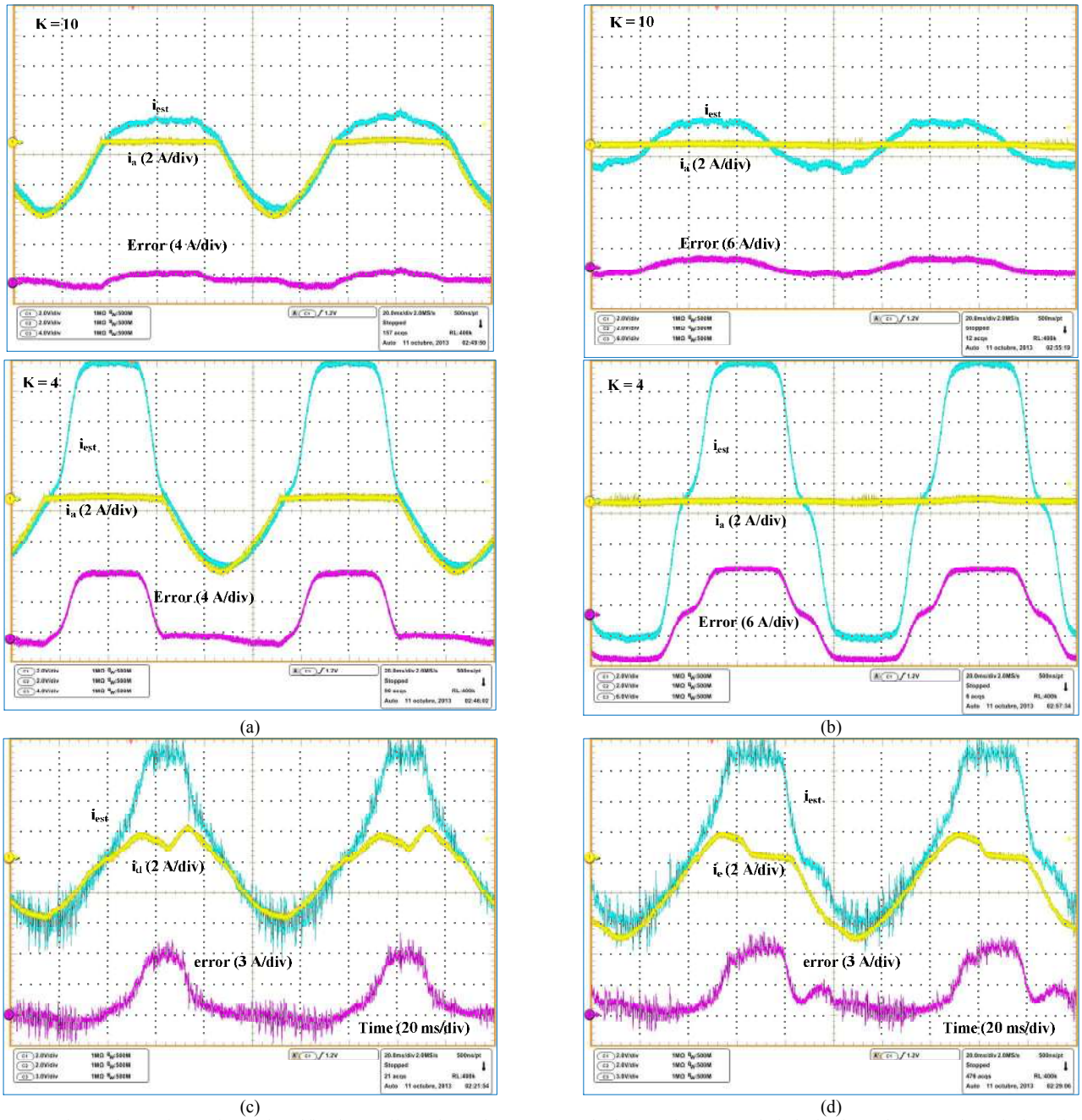

Fig. 7. Experimental waveform of model verification - effect of K value on FD method (a) under open switch fault. (b) under open phase fault. Effect of faulty mode and control on healthy phases (c) under single switch fault. (d) under open phase fault.

B. EXPERIMENTAL RESULTS OF FD

In this section, different faulty modes are considered in the inverter. The proposed FD scheme is used to detect and localize the faulty component.

Robustness to the load transients is an important requirement for a high performance FD method. Considering this, a 75 % step was forced on the motor reference current; experimental results are shown in Fig. 8(a). As it can be seen, FD index *D* is equal to 1, and as a result, no false alarm was generated using the presented method. It should be noted that due to limited number of the oscilloscope channels, here only estimated current, measured current, *D* value and fault signal in phase *a* are shown.

Open switch FD is considered as the second case study; an upper switch fault in phase *a* and a lower switch fault in phase *b* are triggered. The experimental results are shown in Fig. 8(b). As it can be seen, *D* value reduces to zero under faulty modes. In both cases, the fault is detected and localized during less than a quarter of one period.

It is possible to detect open phase faults without using any auxiliary variable. Experimental results of the open phase FD in phase *a* are shown in Fig. 8(c). As it can be seen, *D* value reduces to zero after fault. Fault is detected during less than a quarter of one period.

Since it is possible to operate a five-phase BLDC motor with two faulty phases, the proposed FD method should be able to detect a new fault in a motor with one faulty phase. In this section, the gate signals of phase *a* are removed and motor is operated with fault-tolerant control algorithm adapted for the one faulty phase mode. Subsequently, a new upper switch fault is forced in phase *b*. Experimental results are shown in Fig. 8(d). As it can be seen, the fault is detected and localized successfully.

As explained before, presented FD method is not sensitive to the parameter uncertainty. To validate this capability, resistance value in all phases of the motor model has been decreased 20 %; at the same time, self inductance value has been increased 10 %. An open switch fault and an open phase fault were forced in phase *a*. Experimental results are shown in Figs. 8(e) and (f), respectively. As shown, the fault is detected successfully in both cases.

One remarkable advantage of the presented FD method is its robustness to speed transients. Similar to torque, the speed transients are usual in a variable speed drive for electric vehicles. Therefore, a FD method should also be robust to the speed transients. Here, two experimental results are carried out; in the first case, motor speed is changed from 16 rpm to 23.8 rpm. After that, the motor speed is changed from -23 to 23 rpm. During transients, the parameters of the FD block are not changed. Experimental results are shown in Figs. 8(g) and (h), respectively. As it can be seen, FD technique is robust to the speed transients.

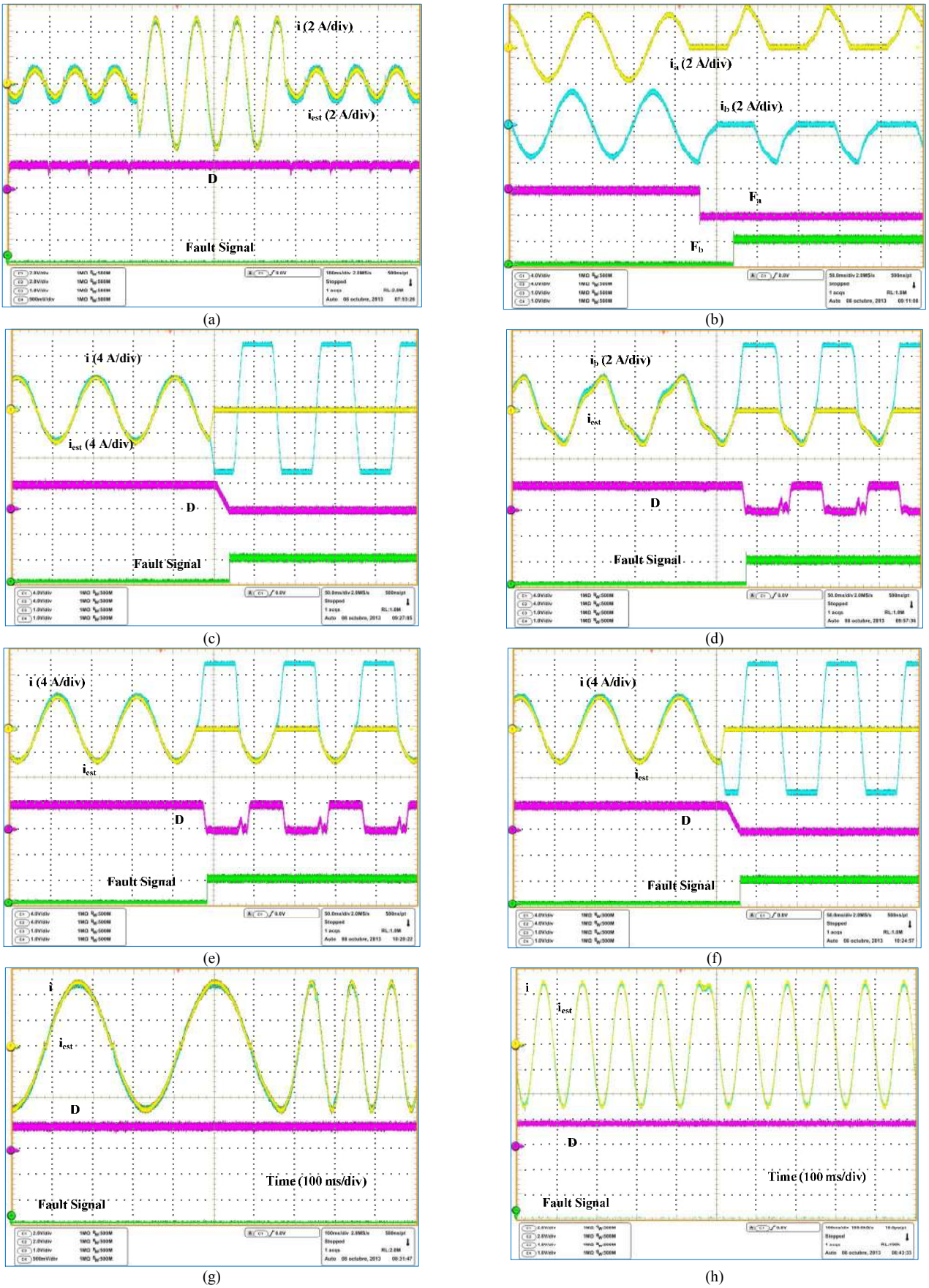

Fig. 8. Experimental waveform of FD (a) Evaluation the effect of load transients. (b) Open switch FD. (c) Open phase FD. (d) FD under faulty mode operation. FD under parameter uncertainty and (e) open switch FD. (f) open phase FD. Evaluate the effect of speed transients. (g) Results under speed variation. (h) Results under speed reverse condition.

C. EXPERIMENTAL RESULTS OF THE FAULT-TOLERANT OPERATION

A high performance FD method should be included in a fault-tolerant control algorithm. The FD block is used in the fault-tolerant control of the five-phase machine to detect the fault. After FD and isolation of the faulty leg, the control method is updated according to the new mode.

In the first step, a fault is started in phase *a*. After FD, the faulty leg is isolated by removing the gate signals in that leg. Healthy mode control is also replaced with faulty mode control. The motor is operated for 5 cycles with the control method for one faulty phase. After that, a new fault is forced in phase *b* which is adjacent to phase *a*. The FD time in phase *b* is less than a quarter of one fundamental cycle. After FD and isolation, control method of the two-adjacent faulty phase mode is used. Experimental results of this mode are shown in Fig. 9. The phase currents i_a, i_b, torque and fault-tolerant code are shown.

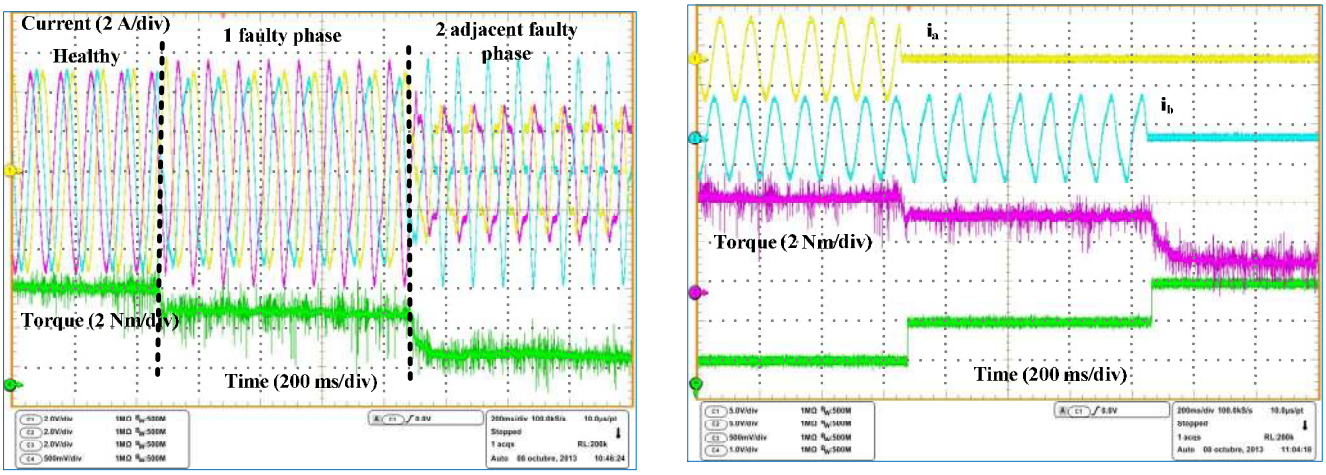

Fig. 9. Experimental waveform of the fault-tolerant control in case of two adjacent faulty phases.

VII. CONCLUSION

A new model based open switch FD technique for two-level VSI is presented in this paper. FD index is based on the cross correlation between the estimated phase currents using SMO and the real currents. By choosing a suitable evaluation period, a robust FD is achieved in less than a quarter of one period. The detection speed is fast. Ability to detect multiple open switch and open phase faults without using auxiliary variable makes this method distinguished from the presented methods in literature. Moreover, the FD index is independent from the load parameters and it is robust against fast transients. In order to design SMO, an observer is used to estimate motor parameters. The estimated parameters are utilized to design the PR controller at the same time. The proposed FD method was applied to a five-phase BLDC motor drive; both detection performance and fault-tolerant capability were evaluated. According to the results, it can detect all open switch faults successfully. Experimental results under fault-tolerant control validate the high efficiency of the proposed FD technique.

REFERENCES

[1] Yantao Song and Bingsen Wang: 'Survey on Reliability of Power Electronic Systems', *IEEE Trans. Power Electron.*, 2013, **28**, (1), pp. 591-604

[2] A. Mohammadpour, S. Sadeghi, and L. Parsa: 'A Generalized Fault-Tolerant Control Strategy for Five-Phase PM Motor Drives Considering Star, Pentagon, and Pentacle Connections of Stator Windings', *IEEE Trans. Ind. Electron.*, 2014, **61**, (1), pp. 63-74

[3] Shaoyong Yang, Angus Bryant, Philip Mawby, Dawei Xiang, Li Ran, and Peter Tavner: 'An Industry-Based Survey of Reliability in Power Electronic Converters', IEEE Trans. Ind. Appl., 2011, **47**, (3), pp. 1441-1451

[4] B. Lu and S. Sharma: 'A literature review of IGBT fault diagnostic and protection methods for power inverters', *IEEE Trans. Ind. Appl.*, 2009, **45**, (5), pp. 1770–1777

[5] M. Shahbazi, P. Poure, S. Saadate, M. R. Zolghadri: 'FPGA-based Fast Detection with Reduced Sensor Count for a Fault-Tolerant Three-Phase Converter', *IEEE Trans. Ind. Informatics*, 2013, **9**, (3), pp. 1343-1350

[6] C. Choi W. Lee: 'Design and evaluation of voltage measurement-based sectoral diagnosis method for inverter open switch faults of permanent magnet synchronous motor drives', *IET Electr. Power Appl.*, 2012, **6**, (8), pp. 526–532

[7] Nuno M. A. Feire, J. O. Estima, and A. J. M. Cardoso: 'Open-Circuit Fault Diagnosis in PMSG Drives for Wind Turbine Applications', *IEEE Trans. Ind. Electron.*, 2013, **60**, (9), pp. 3957-3967

[8] F. Meinguet, P. Sandulescu, X. Kestelyn, and E. Semail: 'A Method for Fault Detection and Isolation based on the Processing of Multiple Diagnostic Indices: Application to Inverter Faults in AC Drives', *IEEE Trans. Veh. Technol.*, 2013, **62**, (3), pp. 995 – 1009

[9] D. Ulises Campos-Delgado, J. Angel Pecina-Sanchez, D. Rivelino Espinoza-Trejo, E. Roman Arce-Santana: 'Diagnosis of open-switch faults in variable speed drives by stator current analysis and pattern recognition', *IET Electr. Power Appl.*, 2013, **7**, (6), pp. 509–522

[10] J. O. Estima and A. J. M. Cardoso: 'A New Algorithm for Real-Time Multiple Open-Circuit Fault Diagnosis in Voltage-Fed PWM Motor Drives by the Reference Current Errors', *IEEE Trans. Ind. Electron.*, 2013, **60**, (8), pp. 3496-3505

[11] D. Rivelino Espinoza-Trejo, D. U. Campos-Delgado, G. Bossio, E. Barcenas, J. E. Hernandez-Diez, L. F. Lugo-Cordero: 'Fault diagnosis scheme for open-circuit faults in field-oriented control induction motor drives', *IET Power Electron.*, 2013, **6**, (5), pp. 869–877

[12] Shin-Myung Jung, Jin-Sik Park, Hag-Wone Kim, Kwan-Yuhl Cho, and Myung-Joong Youn: 'An MRAS-Based Diagnosis of Open-Circuit Fault in PWM Voltage-Source Inverters for PM Synchronous Motor Drive Systems', *IEEE Trans. Power Electron.*, 2013, **28**, (5), pp. 2514-2526

[13] D. R. Espinoza-Trejo, D. U. Campos-Delgado, E. Barcenas, F. J. Martinez-Lopez: 'Robust fault diagnosis scheme for open-circuit faults in voltage source inverters feeding induction motors by using non-linear proportional-integral observers', *IET Power Electron.*, 2012, **5**, (7), pp. 1204–1216

[14] D. U. Campos-Delgado, and D. R. Espinoza-Trejo: 'An Observer- Based Diagnosis Scheme for Single and Simultaneous Open-Switch Faults in Induction Motor Drives', *IEEE Trans. Ind. Electron.*, 2011, **58**, (2), pp. 671-679

[15] Nuno M. A. Freire, Jorge O. Estima, and A. J. Marques Cardoso: 'A Voltage-Based Approach without Extra Hardware for Open-Circuit Fault Diagnosis in Closed-Loop PWM AC Regenerative Drives', *IEEE Trans. Ind. Electron.*, To be Published.

[16] Shuai Shao, Patrick W. Wheeler, Jon C. Clare, and Alan J. Watson: 'Fault detection for Modular Multilevel Converters Based on Sliding Mode Observer', *IEEE Trans. Power Electron.*, 2013, **28**, (11), pp. 4867 – 4872

[17] M. Villani, M. Tursini, G. Fabri, and L. Castellini: 'High Reliability Permanent Magnet Brushless Motor Drive for Aircraft Application', *IEEE Trans. Ind. Electron.*, 2012, **59**, (5), pp. 2073-2081

[18] Taehyun Shim, Sehyun Chang, and Seok Lee: 'Investigation of Sliding-Surface Design on the Performance of Sliding Mode Controller in Antilock Braking Systems', *IEEE Trans. Veh. Technol.*, 2008, **57**, (2), pp. 747-759

[19] Zhaowei Qiao, Tingna Shi, Yindong Wang, Yan Yan, Changliang Xia, and Xiangning He: 'New Sliding-Mode Observer for Position Sensorless Control of Permanent-Magnet Synchronous Motor', *IEEE Trans. Ind. Electron.*, 2013, **60**, (2), pp. 710-719

[20] L. Zarri, M. Mengoni, Y. Gritli, A. Tani, F. Filippetti, G. Serra, and D. Casadei: 'Detection and Localization of Stator Resistance Dissymmetry Based on Multiple Reference Frame Controllers in Multiphase Induction Motor Drives', *IEEE Trans. Ind. Electron.*, 2013, **60**, (8), pp. 3506-3518

[21] Gianluca Gatto, Ignazio Marongiu, and Alessandro Serpi: 'Discrete-Time Parameter Identification of a Surface-Mounted Permanent Magnet Synchronous Machine', *IEEE Trans. Ind. Electron.*, 2013, **60**, (11), pp. 4869-4880

[22] Elhanan Elboher and Michael Werman: 'Asymmetric Correlation: A Noise Robust Similarity Measure for Template Matching', *IEEE Trans. Imag. Process.*, 2013, **22**, (8), pp. 3062-3073

[23] M. Salehifar, R. Salehi Arashloo, J. M. Moreno, V. Sala, L. Romeral: 'Fault Detection and Fault Tolerant Operation of a Five Phase PM Motor Drive Using Adaptive Model Identification Approach', *IEEE Journal of Emerging and Selected Topics on Power Electronics,* 2014, **2**, (2), pp. 212-223

[24] L. Rodrigues Limongi, R. Bojoi, G. Griva, and A. Tenconi: 'Comparing the Performance of Digital Signal Processor-Based Current Controllers for Three-Phase Active Power Filters', *IEEE Ind. Electron. Mag.*, 2009, *Digital Object Identifier 10.1109/MIE.2009.931894*

[25] Yaoqin Jia, Jiqian Zhao, and Xiaowei Fu: 'Direct Grid Current Control of *LCL*-Filtered Grid-Connected Inverter Mitigating Grid Voltage Disturbance', *IEEE Trans. Power Electron.*, 2014, **29**, (3), pp. 1532-1541

[26] A. G. Yepes, F. D. Freijedo, J. Doval-Gandoy, O. Lopez, J. Malvar, and P. Fernandez-Comesana: 'Effects of Discretization Methods on the Performance of Resonant Controllers', *IEEE Trans. Power Electron.*, 2010, **25**, (7), pp. 1692-1712

[27] Chenlei Bao, Xinbo Ruan, Xuehua Wang, Weiwei Li, Donghua Pan, and Kailei Weng: 'Step-by-Step Controller Design for *LCL*-Type Grid-Connected Inverter with Capacitor–Current-Feedback Active-Damping', *IEEE Trans. Power Electron.*, 2014, **29**, (3), pp. 1239-1253

[28] D. G. Holmes, T. A. Lipo, B. P. McGrath, and W. Y. Kong: 'Optimized Design of Stationary Frame Three Phase AC Current Regulators', *IEEE Trans. Power Electron.*, 2009, **24**, (11), pp. 2417-2426

Observer Based Open Transistor Fault Diagnosis and Fault-Tolerant Control of Five-Phase PM Motor Drive for Application in Electric Vehicles

Mehdi SALEHIFAR[1], Ramin Salehi ARASHLOO[2], Manuel MORENO-EGUILAZ[3], Vicent SALA[4], Luis ROMERAL[5]

[1] **CORRESPONDING AUTHOR,** mehdi.salehifar@mcia.upc.edu

[2] ramin.salehi@mcia.upc.edu,

[3] juan.manuel.moreno@mcia.upc.edu

[4] vicent.sala@mcia.upc.edu

[5] Luis.Romeral@mcia.upc.edu

All Authors are with Electronic Engineering Department, UPC, Rambla Sant Nebridi, s/n, 08222 Terrassa, Spain, Tel. +34 633402065, Fax. +34 93 739 89 72

***Abstract* – to meet increasing demand for higher reliability in power electronics converters applicable in electric vehicles, fault detection (FD) is an important part of the control algorithm. In this paper, a model based open transistor fault diagnosis method is presented for a voltage-source inverter (VSI) supplying a five-phase PM motor drive. To realize this goal, a model based observer is designed to estimate model parameters. After that, the estimated parameters are used to design a sliding mode observer (SMO) in order to estimate the phase current in an ideal model. Subsequently, the proposed FD technique measures the similarity between the estimated current and real current using cross correlation factor. This factor is used for the first time in this paper to define a FD index in VSI. The presented FD scheme is simple and fast; also, it is able to detect multiple open switch or open phase faults in contrast to conventional methods. On the other side, in order to track reference current of the motor, the estimated parameters are used to design a proportional resonant (PR) controller. The FD technique is used to operate a multiphase fault-tolerant brushless direct current (BLDC) motor drive. Experimental results on a five-phase BLDC motor with in-wheel outer rotor applicable in electrical vehicles are conducted to validate the theory.**

Keyword – fault diagnosis, multiphase fault-tolerant BLDC motor drive, sliding mode observer, cross correlation.

I. Introduction

Nowadays, power converters are widely used in industrial applications. Along the rising applications, there is an increasing demand for higher reliability provided by the power electronic systems in applications such as transportation, electric and hybrid electric vehicle, space craft, and more electric aircraft. Fault-tolerant concept is an economic solution to meet this requirement [1]. To accomplish a fault-tolerant system, three main subjects should be considered at the same time in the final design including fault-tolerant design, control and fault diagnosis.

Multiphase fault-tolerant permanent magnet (PM) motor drive is a unique solution to achieve high reliability [2]. In the case of a five-phase motor, it is possible to maintain the operation with two faulty phases. Regarding this solution, it is necessary to supply the motor with a fault-tolerant converter. The fault-tolerant converter should be able to detect and isolate the faulty components.

According to a recent survey on reliability of power electronics converters [3], power switches are the most vulnerable components in a power converter among others. A complete review of the faulty modes and detection methods in a power converter was conducted in [4]. Open switch and short circuit faults are the most common faults in a power switch among others. The short circuit fault should be detected and removed quite fast; otherwise it can damage the whole system. Nowadays, hardware based methods are frequently included in commercial gate driver to protect against this fault. On the other side, a solution to detect and protect the open switch fault is not available in commercial products. If it is not detected, secondary faults may happen. Due to growing demand for higher reliability by industry, an extensive research has been conducted on open switch FD methods, recently. Regarding the presented open switch FD methods in literature, these methods can be considered in three different categories including signal based methods, reference based methods and model based methods.

The signal based FD schemes have been extensively studied in literature. To realize a signal based FD method, the current or voltage signal of the power converter can be used as an input to the FD block. The detection methods based on the voltage signal need extra hardware to detect the fault; as a result, implementation of these methods is expensive. However these methods are able to detect the fault very fast. Such schemes have been presented in [5-6].

The FD methods based on the current signal have also been extensively addressed in literature. Different schemes using tools such as Park's vector modulus, wavelet transform, dc current method, normalized dc current method, Fourier transform and slope method have been presented to obtain a suitable FD index [4]. Low detection speed, complexity, inability to detect multiple faults, and sensitivity to fast load transients are the main drawbacks of FD methods based on the current signal. In this category, proposed methods in [7-9] show the highest performance among others.

The second type of the open switch FD method is based on the reference current. According to this method, real current of the converter is measured and compared to the reference current in the control algorithm. After that, a FD index is defined based on

the residue value. This method is cheap, fast and robust to the variations of load parameters. Estima et al. [10] presented a FD method based on the reference current. This method cannot be used in a system with open loop control.

The third type of the open switch FD method is based on the system model. According to this technique, the input signal to the plant is applied to an equivalent mathematical model of the plant, and its response is predicted. In the next step, difference between real output and the predicted signal is used to define the FD index [11-15]. This method is cheap, since extra hardware is not necessary for FD. A FD method based on observer has been presented in [14] to detect multiple open switch faults in a three-phase induction motor. A bank of observers has been proposed to detect the fault. Consequently, implementation of this method will be even more complicated in the case of a multiphase converter. Shao et al. [16] have presented an open switch FD method based on SMO for application in a modular multilevel converter. In order to detect the fault, the residue value (i.e. the difference between estimated and real signal) is compared with a fixed threshold value. This approach can lead to false alarm, since FD index is not independent from load operational conditions.

Regarding the model based FD methods, and to overcome the limitations discussed above, a model based FD method is presented in this paper. Based on this method, in the first step the phase currents are estimated by a full state SMO in a fault-tolerant five-phase BLDC motor drive. Comparing to conventional model based methods which use the residue value (i.e. the difference between measured and estimated state) to define FD index, here cross correlation technique is proposed to define this index. Inputs to the cross correlation technique are the measured and estimated current of the power converter. Proposed method still has the advantages of the conventional methods. At the same time, it can effectively detect multiple open switch or open phase faults. Furthermore, it is quite robust to transients and parameter uncertainties. An estimator is also designed to estimate the motor parameters. The estimated parameters are used for two purposes. These two purposes are SMO design and the PR controller design.

The major contribution of this paper is developing a model based open transistor FD method. To present the FD technique, the remainder of this paper is organized as follows. The model of the five-phase BLDC motor is explained in section II. The current estimation using SMO is presented in section III. Proposed FD scheme is presented in section IV. The FD method is included in a fault-tolerant control algorithm; theory is presented in section V. Proposed FD method is used to detect different faulty modes in a five-phase VSI supplying a BLDC motor; experimental results are shown for both FD and fault-tolerant control in section VI. And finally, the conclusions and remarkable points are presented in section VII.

II. Model of Five-Phase BLDC Motor

The proposed FD technique in this paper intends to implement fault diagnosis in a five-phase VSI supplying a BLDC motor drive, as shown in Fig. 1. Field oriented control (FOC) is used to control the motor; inputs to the control algorithm consist of the phase currents and rotor mechanical position. The same inputs are sent to the FD block. After FD, this block decides the

operation mode (i.e. healthy or faulty) of the motor. In order to isolate the fault, it is necessary to remove the gate signal of the switch in the faulty leg.

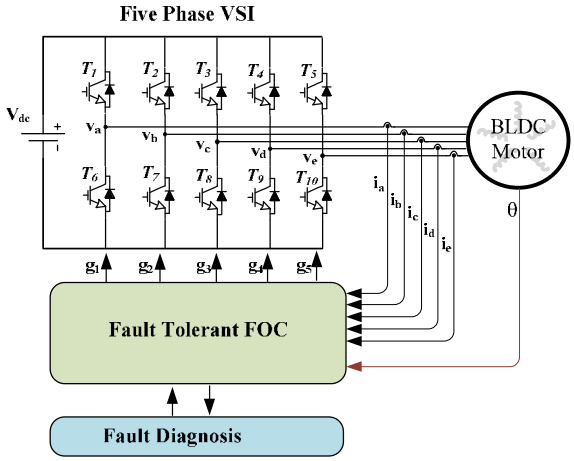

Fig. 1. Fault-Tolerant BLDC motor drive.

To implement FD method, in the first step motor phase currents are estimated based on well-known models. The model in ABCDE reference frame is used due to its less computational requirements and simpler modelling specially under faulty mode. The model of the five-phase BLDC motor with trapezoidal back EMF under healthy and faulty modes is:

$$\begin{bmatrix} v_a \\ v_b \\ v_c \\ v_d \\ v_e \end{bmatrix} = \begin{bmatrix} R_a & 0 & 0 & 0 & 0 \\ 0 & R_b & 0 & 0 & 0 \\ 0 & 0 & R_c & 0 & 0 \\ 0 & 0 & 0 & R_d & 0 \\ 0 & 0 & 0 & 0 & R_e \end{bmatrix} \begin{bmatrix} i_a \\ i_b \\ i_c \\ i_d \\ i_e \end{bmatrix} + \begin{bmatrix} L_a & M_1 & M_2 & M_2 & M_1 \\ M_1 & L_b & M_1 & M_2 & M_2 \\ M_2 & M_1 & L_c & M_1 & M_2 \\ M_2 & M_2 & M_1 & L_d & M_1 \\ M_1 & M_2 & M_2 & M_1 & L_e \end{bmatrix} \frac{d}{dt} \begin{bmatrix} i_a \\ i_b \\ i_c \\ i_d \\ i_e \end{bmatrix} + \begin{bmatrix} e_a \\ e_b \\ e_c \\ e_d \\ e_e \end{bmatrix} - v_x \begin{bmatrix} 1 \\ 1 \\ 1 \\ 1 \\ 1 \end{bmatrix}. \quad (1)$$

where i is the phase current, v is the terminal voltage of each phase, R is the equivalent phase resistance, L is the equivalent phase inductance, M_1 is mutual inductance between two adjacent phases, M_2 is mutual inductance between two nonadjacent phases, e is the back EMF in each phase of the motor, and v_x is the neutral voltage of the motor. The back EMF will be estimated as follows:

$$\begin{bmatrix} e_a \\ e_b \\ e_c \\ e_d \\ e_e \end{bmatrix} = \lambda_{m1}\omega_e \begin{bmatrix} \cos(\vartheta) \\ \cos(\vartheta - 2\pi/5) \\ \cos(\vartheta - 4\pi/5) \\ \cos(\vartheta - 6\pi/5) \\ \cos(\vartheta - 8\pi/5) \end{bmatrix} + \lambda_{m3}\omega_e \begin{bmatrix} \cos(3\vartheta) \\ \cos 3(\vartheta - 2\pi/5) \\ \cos 3(\vartheta - 4\pi/5) \\ \cos 3(\vartheta - 6\pi/5) \\ \cos 3(\vartheta - 8\pi/5) \end{bmatrix}. \quad (2)$$

where λ_{m1} and λ_{m3} are the first and third harmonic amplitudes of the rotor flux linkage; ω_e is the electrical rotational velocity, and Θ is the rotor electrical angle.

To simplify the model under healthy and faulty modes, the model in (1) is redefined in terms of voltage difference between machine terminals as follow:

(3)

$$\begin{bmatrix} v_{ab} \\ v_{bc} \\ v_{cd} \\ v_{de} \end{bmatrix} = \begin{bmatrix} R_a - R_b & 0 & 0 \\ 0 & R_b - R_c & 0 \\ 0 & 0 & R_c & -R_d \\ R_e & R_e & R_e & R_d + R_e \end{bmatrix} \begin{bmatrix} i_a \\ i_b \\ i_c \\ i_d \end{bmatrix} + \begin{bmatrix} e_{ab} \\ e_{bc} \\ e_{cd} \\ e_{de} \end{bmatrix} + \begin{bmatrix} L_a + M_2 - 2M_1 & M_2 - L_b & 2M_2 - 2M_1 & M_2 - M_1 \\ M_1 - M_2 & L_b - M_1 & M_1 - L_c & M_2 - M_1 \\ M_1 - M_2 & 2M_1 - 2M_2 & L_c - M_2 & 2M_1 - M_2 - L_d \\ L_e + M_2 - 2M_1 & L_e - M_1 & L_e - M_2 & L_e + L_d - 2M_1 \end{bmatrix} \frac{d}{dt} \begin{bmatrix} i_a \\ i_b \\ i_c \\ i_d \end{bmatrix}.$$

From design point of view, in order to increase the reliability of a multiphase fault-tolerant machine, the mutual inductances should be minimized [17]. Due to this fact, and because of small effect of mutual inductances given in (1) and (3), this parameter in the model is neglected in the rest of this paper. It should be noted that under faulty mode, the corresponding row and column of the faulty phase are eliminated from (1). After that, the motor model can be simply redefined in terms of voltage difference between machine terminals similar to (3).

The model presented in (3) is utilized to estimate the phase currents and model parameters. The signal estimation methods based on the load model are sensitive to parameter uncertainties and non modeled dynamics [14]. Consequently, to estimate the phase currents accurately, a full state SMO is applied to the open loop model. Due to the observer, the error between real and estimated state variable converges to zero under healthy mode. Details of the designed observer are explained in the next section.

III. Accurate Current Estimation Using SMO

As discussed above, the motor phase currents are estimated based on the motor model. The current estimation is realized using two separate observers. An observer is used to estimate model parameters in (3). Other observer (i.e. SMO) is used to estimate motor phase currents; the estimated motor parameters are used in the SMO. Therefore, the motor model used in the SMO is an ideal model.

If the motor parameters are known accurately, then estimated currents using the open loop model will be equal to the real current. However, these parameters are not easily accessible. On the other hand, parameter values can change with temperature and operational condition of the motor. Furthermore, for condition monitoring and control purposes, it is desirable to calculate machine parameters online.

In order to diagnose the fault and design the PR controllers, the motor parameters are estimated in this paper. Estimation method is explained in the next section.

A. Stator's Parameter Estimation

In a BLDC motor, the stator parameters (i.e. phase resistance and inductance) have a high effect on the accuracy of the open loop model. An estimator is designed to calculate the parameters. The basic equations of the machine model given in (1) can be rewritten as:

$$\frac{d}{dt}i_j = -A_j i_j + B(v_j - e_j), \quad j = a,b,c,d,e. \qquad (4)$$

where $A=R/L$ and $B=1/L$. The goal is to estimate A and B.

In order to improve the estimation accuracy of the open loop model, a nonlinear model reference adaptive observer is designed to estimate the parameters. Estimated currents are as:

$$\frac{d}{dt}\hat{i}_j = -\hat{A}\hat{i}_j + \hat{B}(v_j - e_j), \qquad j = a,b,c,d,e. \qquad (5)$$

where ^ is used to denote the estimated components.

B. STABILITY ANALYSIS

In order to ensure the stability of the estimation algorithm and to design the observers, a stability analysis is done. Here Lyapunov function is used to ensure stability of the system and measurement of parameters. This function is defined as:

$$V = \frac{1}{2}S^2 + \frac{1}{2}(\hat{A}-A)^2 + \frac{1}{2}(\hat{B}-B)^2. \qquad (6)$$

where S is an error function. There are different possibilities to choose the error function [18]. The error function used in this paper is as follows:

$$S = \delta + \lambda\int \delta dt. \qquad (7)$$

where δ is equal to difference between the estimated and real current in each phase of the power converter, and λ is a positive constant. If the error is equal to zero (i.e. S=0), then, the observer is no longer sensitive to parameter uncertainties. Taking into account (1) and (7), the derivative of S for the first element is calculated as:

$$\dot{S} = \dot{\delta} + \lambda\delta. \qquad (8)$$

$$\dot{\delta}_a = \dot{\hat{i}}_a - \dot{i}_a = (A-\hat{A})\dot{\hat{i}}_a - A\delta_a + (v_a - e_a)(\hat{B}-B). \qquad (9)$$

where $\dot{x}$ is equivalent to dx/dt. Similarly, other components are calculated.

According to Lyapunov stability theory, if derivative of V is less than zero for all positive V values, then the system is stable [19]. The derivative of (6) is as:

$$\dot{V} = S^T\dot{S} + (\hat{A}-A)\dot{\hat{A}} + (\hat{B}-B)\dot{\hat{B}}. \qquad (10)$$

From (9) and (10), the derivative of V function can be computed as:

$$\begin{aligned}\dot{V} &= (\delta_a + \lambda\int\delta_a)\times -(A-\lambda)\delta_a \\ &+ ((\delta_a + \lambda\int\delta_a)\times(A-\hat{A})\dot{\hat{i}}_a + (\hat{A}-A)\dot{\hat{A}}) \\ &+ ((\delta_a + \lambda\int\delta_a)\times(v_a - e_a)(\hat{B}-B) + (\hat{B}-B)\dot{\hat{B}}).\end{aligned} \qquad (11)$$

The first element in (11) is negative for λ values less than A. According to Lyapunov stability condition, the remaining components can be calculated as:

$$\dot{\hat{A}} = (\delta_a + \lambda \int \delta_a) \times \hat{i}_a \qquad (12)$$

$$\dot{\hat{B}} = -(\delta_a + \lambda \int \delta_a) \times (v_a - e_a) \qquad (13)$$

Under steady state condition, the error and its dynamic are zero. So, the resistance and inductance can be calculated from (12)-(13) as follows:

$$\frac{1}{\hat{L}} = \frac{1}{L} - \int (\delta_a + \lambda \int \delta_a) \times (v_a - e_a) dt. \qquad (14)$$

$$\hat{R} = R + \hat{L} \int (\delta_a + \lambda \int \delta_a) \times \hat{i}_a. \qquad (15)$$

From (14) and (15), instantaneous values of R and L can be calculated. In this paper, the estimated parameters are used to design the PR controller and to estimate the phase currents using a SMO.

As aforementioned, the estimated parameters can be used for other purposes such as improving the controller of the motor. For example in the case of using a predictive controller in a BLDC motor, it is possible to have both good transient and steady state performance; however the controller performance is sensitive to parameter uncertainties. Therefore, the parameter estimation can be used to design a robust predictive controller. Detection of high resistance connection in cables feeding the machine has been presented in [20], [21].

In order to detect a fault in VSI, the phase currents of the motor are predicted; a SMO is used for this purpose. The estimated parameters in (14)-(15) are used in the SMO. Details of SMO are presented in the following section.

C. Current Estimation

In order to estimate the phase currents, SMO is used in this paper. It has many advantages which make it a suitable option for the state variable estimation. Simple implementation, robustness to parameter uncertainty and measurement noise are the most important factors among others [16].

As it was shown above, a model reference adaptive observer was used to estimate motor parameters. Since real parameters are already known from the parameter estimator, response of the open loop model should be equal to real current. In the case of a healthy motor, error signal reduces to zero after few cycles. In presence of a fault, the model based estimator can no longer estimate the parameters accurately. Under this condition, the error signal increases remarkably.

To detect a fault, the error signal available in SMO is compared to a threshold above zero. If it increases beyond the threshold, a fault alarm is generated. Since the estimated parameters are no longer accurate in a faulty motor, the estimated values are always memorized during one cycle before the fault alarm. After the fault alarm, the controller and model parameters are updated with estimated values for one cycle before the fault.

To estimate the phase currents accurately, the SMO is designed as:

$$\begin{bmatrix} L_a & -L_b & 0 & 0 \\ 0 & L_b & -L_c & 0 \\ 0 & 0 & L_c & -L_d \\ L_e & L_e & L_e & L_e+L_d \end{bmatrix} \frac{d}{dt}\begin{bmatrix} \hat{i}_a \\ \hat{i}_b \\ \hat{i}_c \\ \hat{i}_d \end{bmatrix} = \begin{bmatrix} v_{ab}-e_{ab} \\ v_{bc}-e_{bc} \\ v_{cd}-e_{cd} \\ v_{de}-e_{de} \end{bmatrix} - \begin{bmatrix} R_a & -R_b & 0 & 0 \\ 0 & R_b & -R_c & 0 \\ 0 & 0 & R_c & -R_d \\ R_e & R_e & R_e & R_d+R_e \end{bmatrix}\begin{bmatrix} \hat{i}_a \\ \hat{i}_b \\ \hat{i}_c \\ \hat{i}_d \end{bmatrix} - K \times Sat(\begin{bmatrix} \delta_a \\ \delta_b \\ \delta_c \\ \delta_d \end{bmatrix}). \quad (16)$$

where K is the observer gain, and Sat is a saturation function defined as follows:

$$Sat(x) = \begin{cases} 1 & x \geq 1 \\ x & -1 < x < 1 \\ -1 & x \leq -1 \end{cases} \quad (17)$$

It is possible to use different functions instead of Sat such as $Sigmoid$ and $Sign$ function. The high frequency oscillations can be avoided in the estimated variables, if the saturation function in (17) is used. In order to obtain suitable values of K, a stability analysis is presented in the following section.

To evaluate stability of the SMO, Lyapunov function is defined as:

$$V = \frac{1}{2}S^2. \quad (18)$$

The Lyapunov function and its derivative given in (9)-(10) are similarly adapted here. Taking into account (1) and (18), the derivative of δ for the first element is calculated as:

$$\dot{\hat{\delta}}_a = \dot{\hat{i}}_a - \dot{i}_a = -\frac{R_a}{L_a}(\hat{i}_a - i_a) - \frac{K}{L_a} \times Sat(\hat{i}_a - i_a). \quad (19)$$

Similarly, other components are calculated. So, derivative of V function is as:

$$\dot{V} = [\delta_a \ \delta_b \ \delta_c \ \delta_d \ \delta_e]^T \times \begin{bmatrix} -\frac{R_a}{L_a}\delta_a - \frac{K}{L_a} \times Sat(\delta_a) \\ -\frac{R_b}{L_b}\delta_b - \frac{K}{L_b} \times Sat(\delta_b) \\ -\frac{R_c}{L_c}\delta_c - \frac{K}{L_c} \times Sat(\delta_c) \\ -\frac{R_d}{L_d}\delta_d - \frac{K}{L_d} \times Sat(\delta_d) \\ -\frac{R_e}{L_e}\delta_e - \frac{K}{L_e} \times Sat(\delta_e) \end{bmatrix}. \quad (20)$$

Since Sat function is a linear function, sign of $\delta_a Sat(\delta_a)$ will be always positive. Consequently, the only condition to achieve sliding surface is for positive K values. According to (19), by choosing higher values of K, dynamic behaviour of resultant error will be even faster.

It should be noted that K value has a significant effect on the performance of the proposed FD method. If a very high value is chosen for K, the observed value will follow the real state too fast. Therefore, the residue value will be low. On the other hand, by choosing a small value for K, the estimated current will still follow the current pattern before the fault. In this case, it is easier to detect the fault, since the faulty current is significantly different from the healthy current. A low value of K is an optimal choice in this paper. This assumption results in a robust SMO with slow dynamics. This claim will be later validated with experimental results.

IV. Fault Diagnostic Method

In order to detect the fault, it is possible to define a simple FD index (i.e. the error between the estimated and real current values). Developing this approach for a multiphase machine can lead to false alarms. The main reasons are explained in details in the following.

When a fault occurs in one phase of the converter, closed loop control tries to minimize the error between the reference currents and real currents. As a result, in case that the healthy control method is still applied, output voltage of the control block for a faulty inverter will be changed. On the other hand, in the case of a single switch fault in one phase, a dc value is added to the remaining healthy phase currents. In the case of multiple open switch faults, the dc value can be very high. Consequently, due to effect of the control method, and faulty signals, the estimated currents in the remaining healthy phases can be different from the real values. In addition, simplifications in model can result in a small error. If estimated and real current values are different, this error can be interpreted as a false alarm based on the error value. As a result, FD block should be robust to these cases. These effects will be later validated by experimental results.

To overcome the drawbacks of a simple FD index based on the error function, an alternative solution is proposed in this paper. Here the estimated and measured current signals are fed to a simple unique algorithm. The presented algorithm can detect both the single switch and open phase faults in a VSI. According to this algorithm, the similarity level between two input current signals is measured as a function of time; this measuring factor is known as cross correlation [22]. This factor is defined as:

$$\rho_{x_1-x_2}=\frac{\sum_{j=1}^{N}(x_{1j}-\overline{\mu}_{x1})(x_{2j}-\overline{\mu}_{x2})}{\sqrt{\sum_{j=1}^{N}(x_{1j}-\overline{\mu}_{x1})^2\sum_{j=1}^{N}(x_{2j}-\overline{\mu}_{x2})^2}}. \qquad (21)$$

where x_1 and x_2 are the estimated and measured current in each phase of the power converter, respectively; μ is the moving average value of the input variables and N is the number of samples. It is worth to note that, N value determines the evaluation period in each sampling point. Choosing a small value for N makes the ρ value sensitive to noise. On the other side, a high N value enlarges the detection time. Moreover, the ρ value will be sensitive to frequency transients in a variable speed drive. It

should be noted that the smallest value for N is one sample in one period; the highest value is the number of samples in one period of a fundamental frequency. So, a tradeoff should be done between sensitivity to noise and FD speed.

The ρ value varies from -1 to 1. In the case of completely similar waveforms, its value approaches to 1. According to (21), under healthy condition in a motor drive, both the estimated and real currents are similar, so the correlation factor is near 1. However under faulty mode, these waveforms are quite different at least for half of one fundamental cycle. Under faulty mode, the cross correlation factor reduces to zero. So, the ρ factor is a suitable index to distinguish a healthy condition from a faulty condition.

In comparison to the conventional methods, the proposed method is robust to all false alarms due to fast load transients or unbalanced nonsinusoidal waveforms. Consequently, a FD index is defined as:

$$D = \rho. \qquad (22)$$

The D value is equal to zero under faulty mode, while it is close to 1 under healthy mode. Therefore, D value equal to zero indicates a fault condition. To improve the robustness of the proposed FD method against noise and fast transients, here FD is done with a small time delay denoted by t_d. If the D value is equal to zero during t_d, then the open switch or open phase fault is detected.

After FD, it is necessary to locate the faulty component in VSI. The fault scenario in one leg of VSI can be either a single switch fault or an open phase fault. Due to the single switch fault, average value of the phase current during one fundamental cycle is positive in the case of a lower switch fault or negative in the case of an upper switch fault. In the case of the open phase fault, the phase current and ρ factor are zero. Therefore, fault localization in the case of single switch fault is as:

$$sign(\hat{i}) = \begin{cases} >0 & lower\ switch\ fault \\ <0 & upper\ switch\ fault \end{cases} \qquad (23)$$

Here the estimated current is used to localize the faulty switch. In order to localize the open phase fault, average value of the ρ factor is calculated during one period as:

$$D_{1j} = \frac{1}{M}\sum_{j=1}^{M}\rho_j, \quad j\varepsilon\{a,b,c,d,e\}. \qquad (24)$$

where M is number of samples in one period. If the average value is zero, then the fault type is an open phase fault. For the sake of simplicity, aforementioned fault types are codified. The fault codes are 1, -1 and 2 in the case of upper switch fault, lower switch fault and open phase fault, respectively. These codes are the same in the rest of this paper. Block diagram of the FD method is shown in Fig. 2. In this figure, ε is a small positive value near to zero.

Based on the presented technique, fault localization in the case of a single switch fault is done during one sampling time after FD. Nonetheless, a time delay around one fundamental cycle is necessary to localize the open phase fault. As it can be seen from

Fig. 2, once the fault is detected, fault localization block is enabled. It should be noted that, the FD is done separately in each phase of the power converter. As a result, the presented FD technique can be applied to any two-level multiphase VSI.

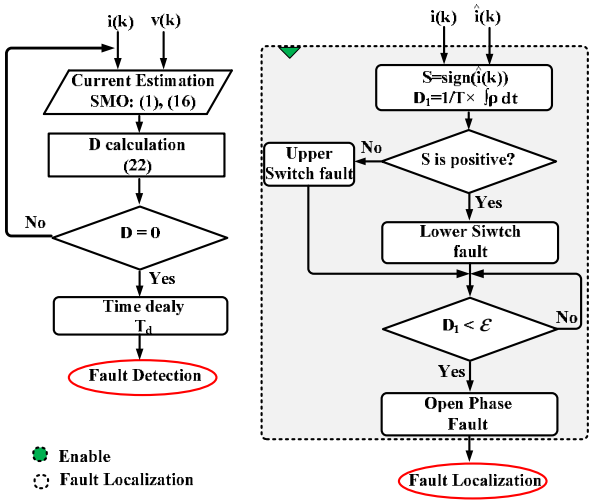

Fig. 2. FD and localization method.

V. Fault-Tolerant Control and Analysis of a Five-Phase BLDC Motor

Application area in this paper is electric vehicles. High reliability is of paramount importance for this application. Five-phase fault-tolerant BLDC motor can meet this requirement. In this paper, fault diagnosis and fault-tolerant control of a multiphase BLDC motor are studied. Block diagram of the studied setup is shown in Fig. 3(a). This motor can be operated with one and two-faulty phases. For clarification, motor operational modes are shown with a code denoted by FC in Fig. 3(a). The operational control mode of the machine is determined by the FD block developed in section IV. Here, control modes of the machine are shown by codes 1, 2, 3, and 4 which correspond to healthy mode, one faulty phase mode, two-adjacent faulty phase mode and two-nonadjacent faulty phase mode, respectively. In the following part, the principals of the fault-tolerant control are briefly reviewed.

In order to control the motor, FOC technique is used. The control algorithm is implemented under healthy and each faulty mode, separately. The basic rules used to calculate the reference currents under different fault conditions were shown in [23]. The calculated reference currents in [23] are shown in Table I. As it can be seen, both first and third harmonics are included in the reference currents. The reference currents are used in this paper in order to realize the fault-tolerant FOC algorithm.

As it can be seen from Fig. 3(a), to implement FOC algorithm, two controllers are used. An outer controller is used to set the motor reference speed shown by ω^*. A proportional-integrator (PI) controller is typically used to realize the speed controller. In addition, an inner controller is used to set the motor reference currents shown by i^*.

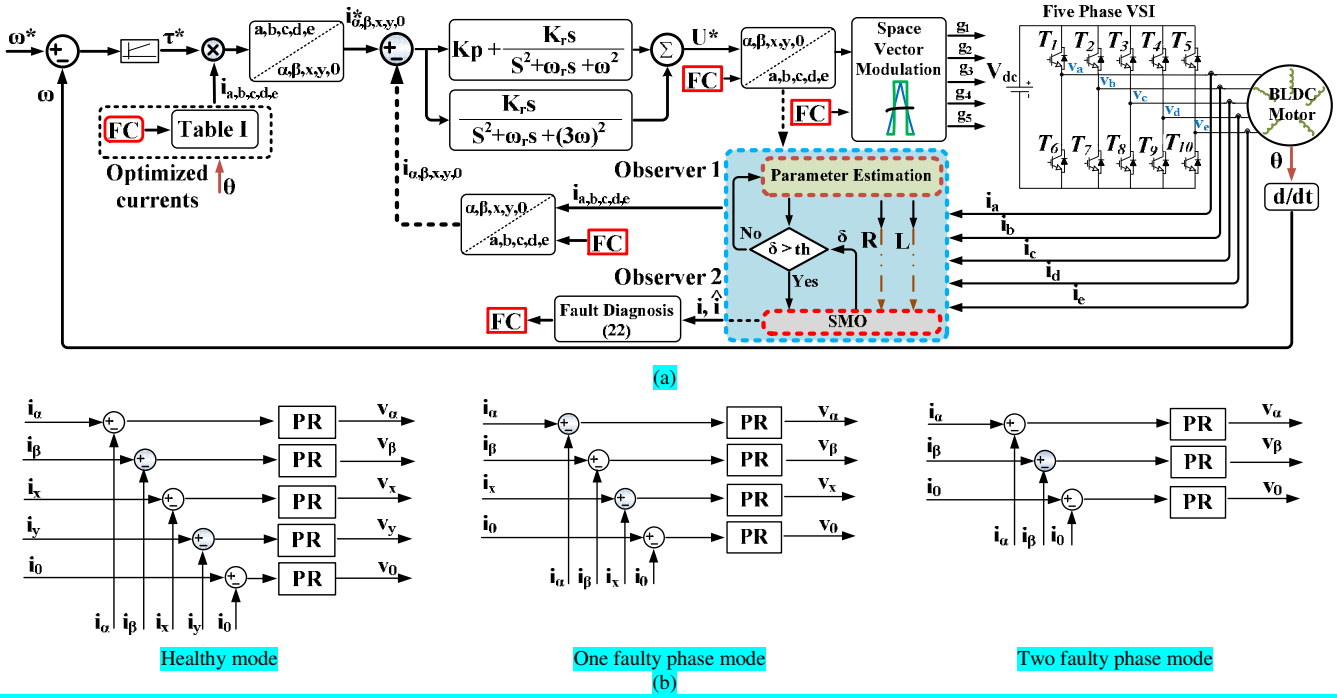

Fig. 3. (a) Fault detection, parameter identification and Fault-Tolerant FOC (b) Block diagram of the inner current controller under each operational mode of the motor.

TABLE I
OPTIMIZED PHASE CURRENTS WITH ISOLATED NEUTRAL

Current	A	B	C	D	E
one faulty phase (FC=2)					
I_1(PU)	0	0.99	0.99	1	0.98
θ_1	-	51	137	232	-41
I_3(PU)	0	0.17	0.08	0.09	0.19
θ_3	-	23	52	186	-19
two adjacent faulty phases (FC=3)					
I_1(PU)	0	0	0.59	0.95	0.67
θ_1	-	-	82	218	0
I_3(PU)	0	0	0.12	0.29	0.16
θ_3	-	-	44	102	41
two nonadjacent faulty phases (FC=4)					
I_1(PU)	0	0.99	0	0.98	0.99
θ_1	-	77	-	2	-42
I_3(PU)	0	0.16	0	0.19	0.17
θ_3	-	15	-	55	-21

The output of the speed controller shown in Fig. 3(a) is the reference torque denoted by τ*. One main assumption to calculate the optimized reference current values in [23] was no ripples in the generated torque. Therefore, authors here use the conventional PI control to set the reference speed.

Inner controller can be done in different ways. A comprehensive study has been done on different current controllers in [24]. *PI* controller in synchronous reference frame and *PR* controller in stationary reference frame are two possible control methods to set the reference currents. Regarding the optimized reference currents given in table I, under faulty mode, the phase currents are unbalanced and nonsinusoidal. In the case of using a simple *PI* controller, due to unbalanced nonsinusoidal phase currents, both dc component and oscillatory components appear in reference currents after transferring to synchronous reference frame. In order

to have dc reference currents, *PI* controller should be designed separately for positive and negative sequence components. This implies high computational cost and complicated controller design. Furthermore, *PI* controller should be able to track harmonic components as well. It is known in literature that *PI* controller has a high performance to track dc components [24], [25]. In the case of sinusoidal components; there will be steady state error. Therefore, the second disadvantage of *PI* control is poor tracking performance due to its limited bandwidth.

As shown in Fig. 3(a), in this paper, *PR* controller in stationary reference frame is used to implement the inner current controller. According to [24], this controller is able to set both positive and negative sequence components at the same time. On the other hand, resonant controllers can be set individually to track each desired harmonic component. In order to track the reference currents in a five-phase BLDC motor, *PR* controller should be able to control both the first and third harmonics.

Transfer function of *PR* controller is as:

$$G_c(s) = K_p + \frac{K_r s}{s^2 + \omega_r s + \omega_o^2} + \frac{K_r s}{s^2 + \omega_r s + (3\omega_o)^2} \quad (25)$$

where $\omega_o=2\pi f_o$, and f_o is the resonance frequency of the controller, K_p is the proportional gain, K_r is the resonant gain, and ω_r is the bandwidth of the controller around the resonance frequency. It should be noted that ω_r is used to reduce the controller sensitivity at resonance frequency. This criterion should be considered in variable speed drives due to speed variations of the motor. Also, f_o is determined from the motor speed.

As aforementioned, a five-phase BLDC motor can be operated with two faulty phases. This means that inverter configuration under healthy mode, one faulty phase mode, and two faulty phase mode are the five-phase, four-phase, and three-phase, respectively. So, the inner current controller should be reconfigured under each operational mode of the machine. The inner current control scheme at each mode is shown in Fig. 3(b). It should be noted that the Park's transformation should also be updated for five-phase, four-phase or three-phase currents at each operational mode of the machine.

VI. Experimental Results

To validate the theory, experimental results are conducted on a five-phase BLDC motor as shown in Fig. 4. As it can be seen, the five-phase motor is coupled with a commercial three-phase permanent magnet synchronous motor (PMSM) which serves as the load motor. The load motor is supplied with an independent AC SIEMENS drive (known as SINAMICS-S120). A national instrument card known as Compactrio is used as interface between the three phase PMSM drive and the host PC. The torque and speed references of the load motor can be set from the host PC. The five-phase motor parameters are shown in table II. It has an outer rotor in-wheel structure; this configuration is useful for electric vehicles. The control algorithm, and FD method of the five-phase motor are implemented in a dSPACE control board model ds1005. The motor is supplied with a five-phase two level VSI.

The sampling frequency of the phase currents is 4 kHz. The dc link voltage of the VSI is 24 V and its switching frequency is 4 kHz. Motor speed is 23.8 rpm, and rated frequency of the phase currents is 10 Hz.

The experimental results are presented in three sections. In the first section, the motor model is tuned with estimated parameters. After that, the effect of K value on FD performance is discussed. Moreover, characteristics of FD method for application in a multiphase machine will be explained. In the second section, different faulty types are implemented in the inverter; FD method is used to detect and localize the faults. In the last section, the fault-tolerant control of a five-phase BLDC motor is presented; here the FD block is used to achieve the fault-tolerant operation.

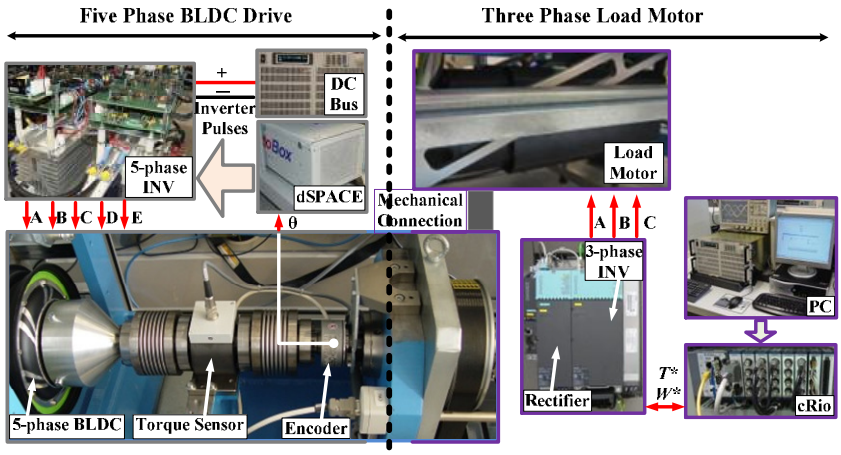

Fig. 4. Experimental setup.

TABLE II
MOTOR PARAMETERS

Number of Pole Pairs		26
Stator Resistance		0.1 Ω
Stator Inductance	L_{aa}	408 μH
	L_{ab}	15 μH
	L_{ac}	18 μH
Nominal Torque		8 Nm
Nominal Speed		400 rpm
Permanent Magnet Flux		0.0178 Wb
Moment of Inertia		0.0583 kgm^2

A. Model Verification

In order to tune the open loop model, in the first step, the presented algorithm in section III is implemented to estimate the stator resistance and inductance of the five-phase BLDC motor. The estimated parameters during four fundamental cycles are shown in Fig. 5(a). As it can be seen, the resistance and inductance value are 0.75 Ω and 490 μH, respectively. To validate effectiveness of the developed theory, a 0.25 Ω resistance was connected in series with phase a. After a short time, it is short circuited. Experimental result of the stator resistance estimation is shown in Fig. 5(b). As it can be seen, the presented parameter estimator can accurately measure the added value.

In the second step, after parameter estimation, the calculated values are used to design the PR controller. Details of the controller design are discussed in the following.

Different methods have been presented in literature to design the PR controllers. In comparison to PI controller, here by adding a resonance term in parallel to a proportional term, the frequency response is only affected around the resonance frequency. The bandwidth of the controller given in (25) at the resonance frequency is defined by integrator term. The proportional gain can be designed similar to *PI* controllers. A similar gain can be chosen for both the first and third harmonics [26]. As a result, the controller design is only considered for the first harmonic.

In order to eliminate the high frequency noise, and at the same time to have a fast dynamic response, the cut off frequency shown by ω_c in this paper is determined well above the resonance frequency [27]. Typical applications consider 1/5 of the switching frequency as the design specification. On the other side, to reduce the controller sensitivity around the resonance frequency, the ω_r value in (25) should be different from zero. In this paper, the design specification is to set ω_r at 0.0628 rad/s, and ω_c at 600 Hz.

Using the estimated parameters, the PR controller is designed according the design method presented in [28]. A block diagram of the inner current controller is shown in Fig. 6(a). Regarding the controller design specifications, the phase margin was considered higher than 45 degrees. Limited value of the motor operation speed for experimental setup is considered as 50 rpm; frequency of the motor phase current at this speed is 21.6 Hz. The designed values for K_p, K_r are 0.067, and 25.27, respectively. The frequency response of the designed PR controller is shown in Fig. 6(b). As it can be seen, the controller has a high gain at the resonance frequency. Therefore, the controller can effectively track both the first and third harmonic components of the motor phase current.

In the third step, the effect of K value on FD algorithm is evaluated. two case studies are considered for different values of K. For the first case, single switch FD is studied for a low and a high K value. Experimental results are shown in Fig. 7(a). The estimated current, real current and error signal are shown. As it can be seen, for small K values, the error signal is significantly high. For the second case, open phase FD is evaluated. The final waveforms are shown in Fig. 7(b). As it can be seen, in case of small K value, the error signal is high. Consequently, a low value of K equal to 4 is considered in this paper which is the same in the rest of this paper.

As discussed before, faulty signals, inaccurate model, and control method performance can affect the estimated current in the remaining healthy phases. To validate this claim, two faulty scenarios are considered here. In the first case, an open switch fault in phase a, and an open phase fault in phase b are considered. The estimated current, real current and error value in phase d are shown in Fig. 7(c). As it can be seen, regardless of being a healthy phase, there is a dc value in phase d current. At the same time, the error value during half of one period is high. If the error is used as the FD index, false alarms can be generated in this phase.

To further validate this claim, three lower switch faults are considered in phases *a*, *b*, and *c*. The phase *e* current and error value are shown in Fig. 7(d). Although there is no fault in this phase, the estimated and real current are different.

The presented analysis validates the necessity of a high performance FD method which is robust to these effects. As described above, the FD index presented in (22) in this paper has this characteristic.

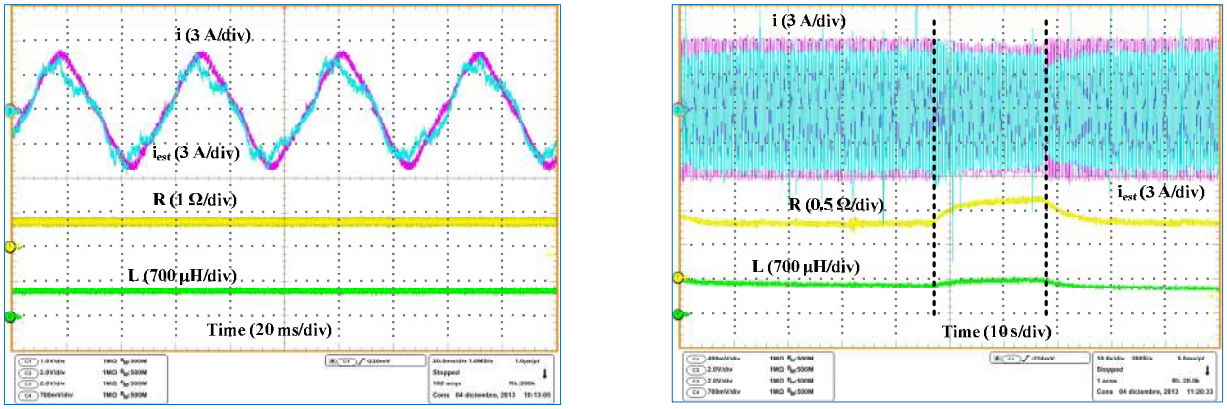

(a) (b)

Fig. 5. Estimated resistance of the stator. (a) Results during four cycles. (b) Results for long time.

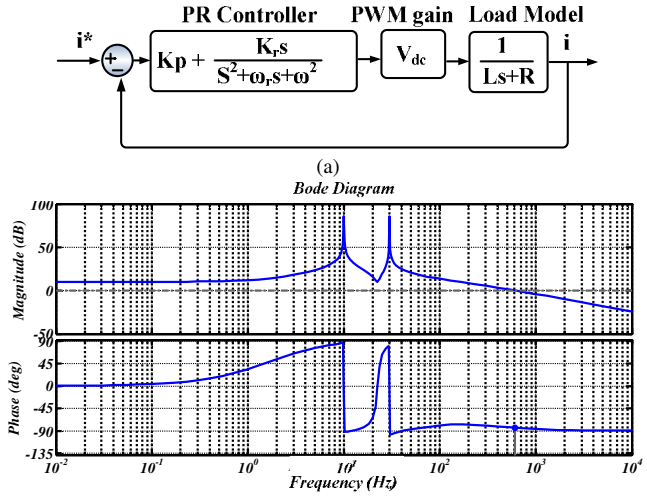

(a)

(b)

Fig. 6. (a) Block diagram of the current controller (b) frequency of the current controller and its frequency response at ω_c=3768 (rad/sec), ω_r=0.0628 (rad/sec) and ω_o=62.8 (rad/sec).

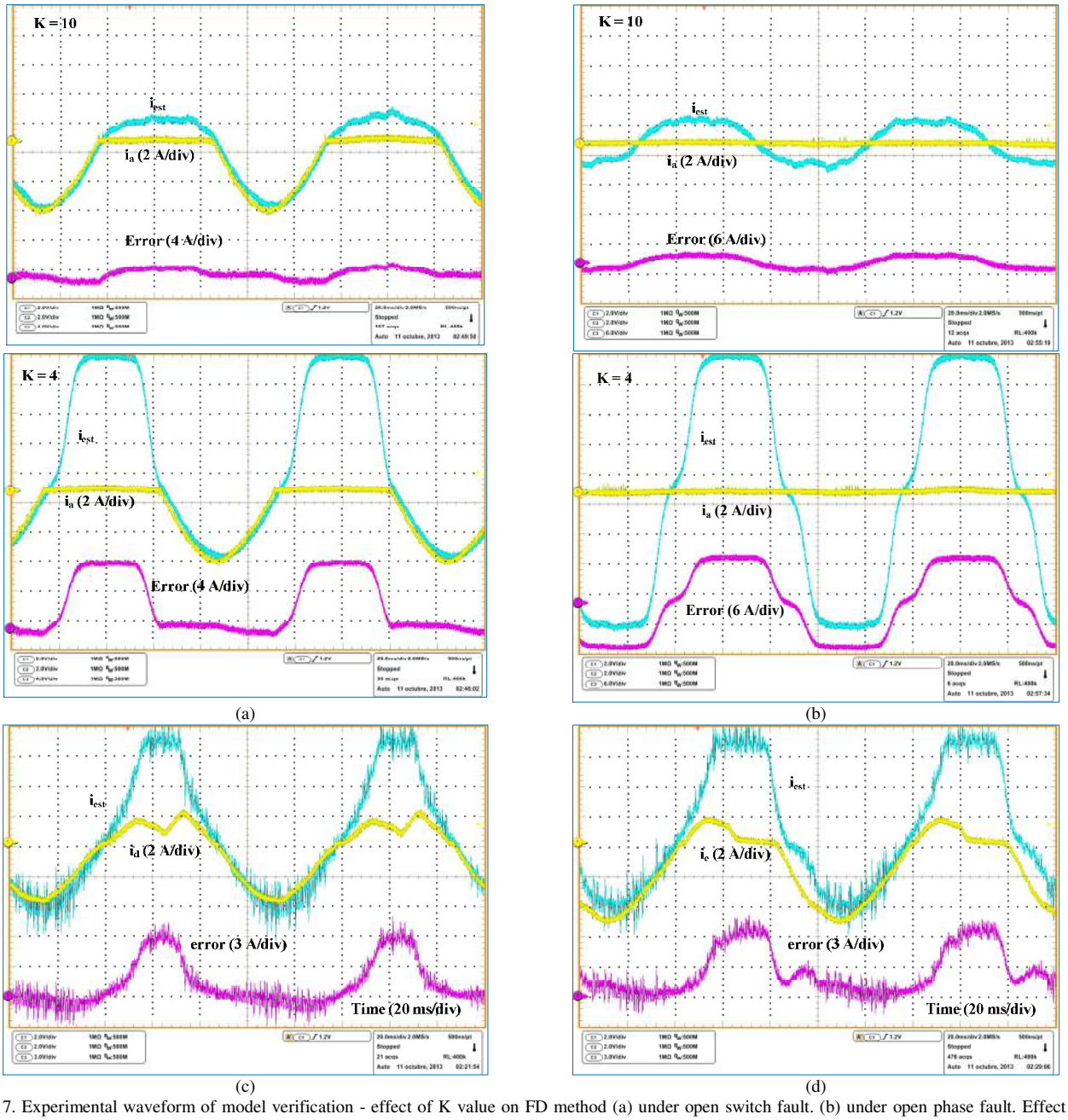

Fig. 7. Experimental waveform of model verification - effect of K value on FD method (a) under open switch fault. (b) under open phase fault. Effect of faulty mode and control on healthy phases (c) under single switch fault. (d) under open phase fault.

B. EXPERIMENTAL RESULTS OF FD

In this section, different faulty modes are considered in the inverter. The proposed FD scheme is used to detect and localize the faulty component.

Robustness to the load transients is an important requirement for a high performance FD method. Considering this, a 75 % step was forced on the motor reference current; experimental results are shown in Fig. 8(a). As it can be seen, FD index *D* is equal to 1, and as a result, no false alarm was generated using the presented method. It should be noted that due to limited number of the oscilloscope channels, here only estimated current, measured current, *D* value and fault signal in phase *a* are shown.

Open switch FD is considered as the second case study; an upper switch fault in phase *a* and a lower switch fault in phase *b* are triggered. The experimental results are shown in Fig. 8(b). As it can be seen, *D* value reduces to zero under faulty modes. In both cases, the fault is detected and localized during less than a quarter of one period.

It is possible to detect open phase faults without using any auxiliary variable. Experimental results of the open phase FD in phase *a* are shown in Fig. 8(c). As it can be seen, *D* value reduces to zero after fault. Fault is detected during less than a quarter of one period.

Since it is possible to operate a five-phase BLDC motor with two faulty phases, the proposed FD method should be able to detect a new fault in a motor with one faulty phase. In this section, the gate signals of phase *a* are removed and motor is operated with fault-tolerant control algorithm adapted for the one faulty phase mode. Subsequently, a new upper switch fault is forced in phase *b*. Experimental results are shown in Fig. 8(d). As it can be seen, the fault is detected and localized successfully.

As explained before, presented FD method is not sensitive to the parameter uncertainty. To validate this capability, resistance value in all phases of the motor model has been decreased 20 %; at the same time, self inductance value has been increased 10 %. An open switch fault and an open phase fault were forced in phase *a*. Experimental results are shown in Figs. 8(e) and (f), respectively. As shown, the fault is detected successfully in both cases.

One remarkable advantage of the presented FD method is its robustness to speed transients. Similar to torque, the speed transients are usual in a variable speed drive for electric vehicles. Therefore, a FD method should also be robust to the speed transients. Here, two experimental results are carried out; in the first case, motor speed is changed from 16 rpm to 23.8 rpm. After that, the motor speed is changed from -23 to 23 rpm. During transients, the parameters of the FD block are not changed. Experimental results are shown in Figs. 8(g) and (h), respectively. As it can be seen, FD technique is robust to the speed transients.

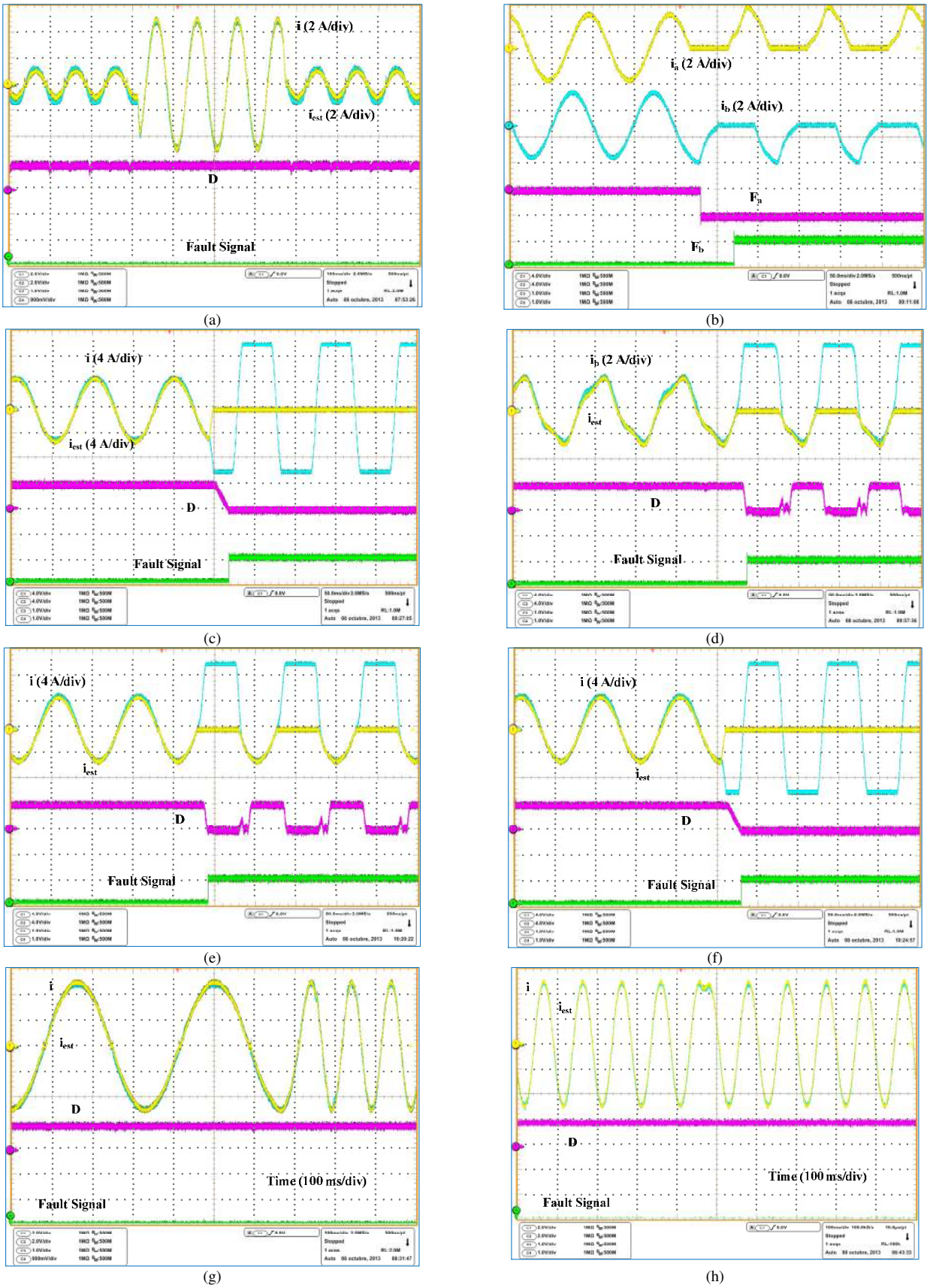

Fig. 8. Experimental waveform of FD (a) Evaluation the effect of load transients. (b) Open switch FD. (c) Open phase FD. (d) FD under faulty mode operation. FD under parameter uncertainty and (e) open switch FD. (f) open phase FD. Evaluate the effect of speed transients. (g) Results under speed variation. (h) Results under speed reverse condition.

C. EXPERIMENTAL RESULTS OF THE FAULT-TOLERANT OPERATION

A high performance FD method should be included in a fault-tolerant control algorithm. The FD block is used in the fault-tolerant control of the five-phase machine to detect the fault. After FD and isolation of the faulty leg, the control method is updated according to the new mode.

In the first step, a fault is started in phase *a*. After FD, the faulty leg is isolated by removing the gate signals in that leg. Healthy mode control is also replaced with faulty mode control. The motor is operated for 5 cycles with the control method for one faulty phase. After that, a new fault is forced in phase *b* which is adjacent to phase *a*. The FD time in phase *b* is less than a quarter of one fundamental cycle. After FD and isolation, control method of the two-adjacent faulty phase mode is used. Experimental results of this mode are shown in Fig. 9. The phase currents i_a, i_b, torque and fault-tolerant code are shown.

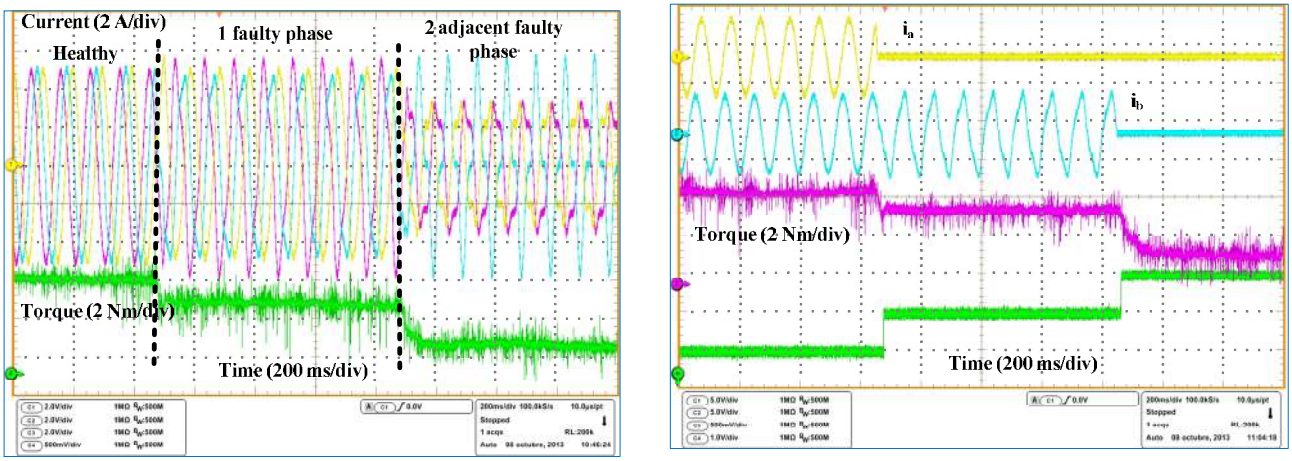

Fig. 9. Experimental waveform of the fault-tolerant control in case of two adjacent faulty phases.

VII. CONCLUSION

A new model based open switch FD technique for two-level VSI is presented in this paper. FD index is based on the cross correlation between the estimated phase currents using SMO and the real currents. By choosing a suitable evaluation period, a robust FD is achieved in less than a quarter of one period. The detection speed is fast. Ability to detect multiple open switch and open phase faults without using auxiliary variable makes this method distinguished from the presented methods in literature. Moreover, the FD index is independent from the load parameters and it is robust against fast transients. In order to design SMO, an observer is used to estimate motor parameters. The estimated parameters are utilized to design the PR controller at the same time. The proposed FD method was applied to a five-phase BLDC motor drive; both detection performance and fault-tolerant capability were evaluated. According to the results, it can detect all open switch faults successfully. Experimental results under fault-tolerant control validate the high efficiency of the proposed FD technique.

REFERENCES

[1] Yantao Song and Bingsen Wang: 'Survey on Reliability of Power Electronic Systems', *IEEE Trans. Power Electron.*, 2013, **28**, (1), pp. 591-604

[2] A. Mohammadpour, S. Sadeghi, and L. Parsa: 'A Generalized Fault-Tolerant Control Strategy for Five-Phase PM Motor Drives Considering Star, Pentagon, and Pentacle Connections of Stator Windings', *IEEE Trans. Ind. Electron.*, 2014, **61**, (1), pp. 63-74

[3] Shaoyong Yang, Angus Bryant, Philip Mawby, Dawei Xiang, Li Ran, and Peter Tavner: 'An Industry-Based Survey of Reliability in Power Electronic Converters', IEEE Trans. Ind. Appl., 2011, **47**, (3), pp. 1441-1451

[4] B. Lu and S. Sharma: 'A literature review of IGBT fault diagnostic and protection methods for power inverters', *IEEE Trans. Ind. Appl.*, 2009, **45**, (5), pp. 1770–1777

[5] M. Shahbazi, P. Poure, S. Saadate, M. R. Zolghadri: 'FPGA-based Fast Detection with Reduced Sensor Count for a Fault-Tolerant Three-Phase Converter', *IEEE Trans. Ind. Informatics*, 2013, **9**, (3), pp. 1343-1350

[6] C. Choi W. Lee: 'Design and evaluation of voltage measurement-based sectoral diagnosis method for inverter open switch faults of permanent magnet synchronous motor drives', *IET Electr. Power Appl.*, 2012, **6**, (8), pp. 526–532

[7] Nuno M. A. Feire, J. O. Estima, and A. J. M. Cardoso: 'Open-Circuit Fault Diagnosis in PMSG Drives for Wind Turbine Applications', *IEEE Trans. Ind. Electron.*, 2013, **60**, (9), pp. 3957-3967

[8] F. Meinguet, P. Sandulescu, X. Kestelyn, and E. Semail: 'A Method for Fault Detection and Isolation based on the Processing of Multiple Diagnostic Indices: Application to Inverter Faults in AC Drives', *IEEE Trans. Veh. Technol.*, 2013, **62**, (3), pp. 995 – 1009

[9] D. Ulises Campos-Delgado, J. Angel Pecina-Sanchez, D. Rivelino Espinoza-Trejo, E. Roman Arce-Santana: 'Diagnosis of open-switch faults in variable speed drives by stator current analysis and pattern recognition', *IET Electr. Power Appl.*, 2013, **7**, (6), pp. 509–522

[10] J. O. Estima and A. J. M. Cardoso: 'A New Algorithm for Real-Time Multiple Open-Circuit Fault Diagnosis in Voltage-Fed PWM Motor Drives by the Reference Current Errors', *IEEE Trans. Ind. Electron.*, 2013, **60**, (8), pp. 3496-3505

[11] D. Rivelino Espinoza-Trejo, D. U. Campos-Delgado, G. Bossio, E. Barcenas, J. E. Hernandez-Diez, L. F. Lugo-Cordero: 'Fault diagnosis scheme for open-circuit faults in field-oriented control induction motor drives', *IET Power Electron.*, 2013, **6**, (5), pp. 869–877

[12] Shin-Myung Jung, Jin-Sik Park, Hag-Wone Kim, Kwan-Yuhl Cho, and Myung-Joong Youn: 'An MRAS-Based Diagnosis of Open-Circuit Fault in PWM Voltage-Source Inverters for PM Synchronous Motor Drive Systems', *IEEE Trans. Power Electron.*, 2013, **28**, (5), pp. 2514-2526

[13] D. R. Espinoza-Trejo, D. U. Campos-Delgado, E. Barcenas, F. J. Martinez-Lopez: 'Robust fault diagnosis scheme for open-circuit faults in voltage source inverters feeding induction motors by using non-linear proportional-integral observers', *IET Power Electron.*, 2012, **5**, (7), pp. 1204–1216

[14] D. U. Campos-Delgado, and D. R. Espinoza-Trejo: 'An Observer- Based Diagnosis Scheme for Single and Simultaneous Open-Switch Faults in Induction Motor Drives', *IEEE Trans. Ind. Electron.*, 2011, **58**, (2), pp. 671-679

[15] Nuno M. A. Freire, Jorge O. Estima, and A. J. Marques Cardoso: 'A Voltage-Based Approach without Extra Hardware for Open-Circuit Fault Diagnosis in Closed-Loop PWM AC Regenerative Drives', *IEEE Trans. Ind. Electron.*, To be Published.

[16] Shuai Shao, Patrick W. Wheeler, Jon C. Clare, and Alan J. Watson: 'Fault detection for Modular Multilevel Converters Based on Sliding Mode Observer', *IEEE Trans. Power Electron.*, 2013, **28**, (11), pp. 4867 – 4872

[17] M. Villani, M. Tursini, G. Fabri, and L. Castellini: 'High Reliability Permanent Magnet Brushless Motor Drive for Aircraft Application', *IEEE Trans. Ind. Electron.*, 2012, **59**, (5), pp. 2073-2081

[18] Taehyun Shim, Sehyun Chang, and Seok Lee: 'Investigation of Sliding-Surface Design on the Performance of Sliding Mode Controller in Antilock Braking Systems', *IEEE Trans. Veh. Technol.*, 2008, **57**, (2), pp. 747-759

[19] Zhaowei Qiao, Tingna Shi, Yindong Wang, Yan Yan, Changliang Xia, and Xiangning He: 'New Sliding-Mode Observer for Position Sensorless Control of Permanent-Magnet Synchronous Motor', *IEEE Trans. Ind. Electron.*, 2013, **60**, (2), pp. 710-719

[20] L. Zarri, M. Mengoni, Y. Gritli, A. Tani, F. Filippetti, G. Serra, and D. Casadei: 'Detection and Localization of Stator Resistance Dissymmetry Based on Multiple Reference Frame Controllers in Multiphase Induction Motor Drives', *IEEE Trans. Ind. Electron.*, 2013, **60**, (8), pp. 3506-3518

[21] Gianluca Gatto, Ignazio Marongiu, and Alessandro Serpi: 'Discrete-Time Parameter Identification of a Surface-Mounted Permanent Magnet Synchronous Machine', *IEEE Trans. Ind. Electron.*, 2013, **60**, (11), pp. 4869-4880

[22] Elhanan Elboher and Michael Werman: 'Asymmetric Correlation: A Noise Robust Similarity Measure for Template Matching', *IEEE Trans. Imag. Process.*, 2013, **22**, (8), pp. 3062-3073

[23] M. Salehifar, R. Salehi Arashloo, J. M. Moreno, V. Sala, L. Romeral: 'Fault Detection and Fault Tolerant Operation of a Five Phase PM Motor Drive Using Adaptive Model Identification Approach', *IEEE Journal of Emerging and Selected Topics on Power Electronics,* 2014, **2**, (2), pp. 212-223

[24] L. Rodrigues Limongi, R. Bojoi, G. Griva, and A. Tenconi: 'Comparing the Performance of Digital Signal Processor-Based Current Controllers for Three-Phase Active Power Filters', *IEEE Ind. Electron. Mag.*, 2009, *Digital Object Identifier 10.1109/MIE.2009.931894*

[25] Yaoqin Jia, Jiqian Zhao, and Xiaowei Fu: 'Direct Grid Current Control of *LCL*-Filtered Grid-Connected Inverter Mitigating Grid Voltage Disturbance', *IEEE Trans. Power Electron.*, 2014, **29**, (3), pp. 1532-1541

[26] A. G. Yepes, F. D. Freijedo, J. Doval-Gandoy, O. Lopez, J. Malvar, and P. Fernandez-Comesana: 'Effects of Discretization Methods on the Performance of Resonant Controllers', *IEEE Trans. Power Electron.*, 2010, **25**, (7), pp. 1692-1712

[27] Chenlei Bao, Xinbo Ruan, Xuehua Wang, Weiwei Li, Donghua Pan, and Kailei Weng: 'Step-by-Step Controller Design for *LCL*-Type Grid-Connected Inverter with Capacitor–Current-Feedback Active-Damping', *IEEE Trans. Power Electron.*, 2014, **29**, (3), pp. 1239-1253

[28] D. G. Holmes, T. A. Lipo, B. P. McGrath, and W. Y. Kong: 'Optimized Design of Stationary Frame Three Phase AC Current Regulators', *IEEE Trans. Power Electron.*, 2009, **24**, (11), pp. 2417-2426